POLITECNICO DI TORINO

Master's Degree in Aerospace Engineering

Master's Degree Thesis

Optimization of hybrid rocket motors for small launchers' upper-stage

Supervisor
Prof. Lorenzo Casalino

Candidate
Andrea Mammola

October 2020

Ringrazio in primo luogo il relatore della tesi Prof. Lorenzo Casalino per la Sua cortesia e disponibilità nel fornire chiarimenti.
Un ringraziamento speciale va alla mia fidanzata Marzia che è sempre stata un punto di riferimento durante tutto il percorso universitario.
Con riconoscenza per il sostegno fornitomi durante gli studi ringrazio i miei genitori Silvia e Riccardo, le mie nonne Fernanda e Marcella, mio fratello Davide e i miei due nonni Antonino e Paolo che, nonostante non ci siano più, ricordo con orgoglio e gratitudine.

I thank primarily the supervisor of the thesis Prof. Lorenzo Casalino for his courtesy and availability in providing clarifications.
Special thanks go to my girlfriend Marzia who has always been a point of reference throughout my university career.
With thankfulness for the support given to me during my studies, I thank my parents Silvia and Riccardo, my grandmothers Fernanda and Marcella, my brother Davide and my two grandfathers Antonino and Paolo who, even though they are gone, I remember with pride and gratitude.

Abstract

The study of rocket engines and motors has become fundamental during last years. In particular the simple idea of “space exploration”, with its political power, has been joined by other more economic aspects. Telecommunications industry and research institutions are increasingly oriented towards the development of new satellites. That’s why the private industry of launchers is growing more and more, creating a new important market. The necessity of powerful, efficient, environmentally friendly, cheap and safe rockets is the new target in order to send into orbit the heaviest payload at the minimum cost. Just the small launchers (up to 2000 kg payload in LEO) industry needs nowadays new solutions, so far little considered, to be optimized. In particular the frontier of hybrid rockets allows a new approach to propellant combustion that could be revolutionary for future commercial space flights.

The thesis work here reported analyses the small launcher *Vega*, actually in use, modifying the 3rd solid and 4th liquid stage with a unique hybrid upper-stage. The hybrid rocket motor (HRM) described uses a solid grain of fuel and a liquid oxidizer, whose tank has a feed system with partially regulated pressure. The throttle control through the liquid oxidizer mass flow should be possible, but it’s not used because it would need some heavy and expensive control systems (e.g. aft-end injector and mixer). This new type of solution for a rocket motor upper-stage is cheaper, lighter and simpler than the previous one, despite the typical HRM’s problems like mixture ratio shifting and low combustion efficiency. The goal of the work is to implement a new mission with some constraints (resizing of *Vega*) and to optimize the motor parameters in order to maximize the payload and to place it into a 500 km orbit. This is possible with a code developed by *Politecnico di Torino* and written in *Fortran* programming language, which realizes a coupled optimization of motor design (direct method used) and trajectory (indirect approach based on thrust direction and motor switching times).

The thesis paper is divided into different sections. The *chapter 1* in the first part describes the general subdivision of rocket motors and engines, focusing on the HRM, while in the second part outlines the characteristics of *Vega* and its mission phases. The next section deals with the analysis of the Vega’s new solution with a HRM upper-stage, and the comprehension of the *Fortran* code, dwelling on the subroutine dedicated to mass budget (*chapter 2*). The last part (*chapter 3*) describes in detail the work done to achieve the final optimization and to obtain the results, illustrated in tables and plots.

Index

Chapter 1

Introduction

Rockets are the best way to realize space explorations. During the last years the space business became fundamental: the actual target is not only the exploration, but also the satellites' service supply (telecommunications, scientific research, etc.), which has a not negligible economic impact especially on the private industry. For this reason the research never stopped, looking for improvements in term of cost, performance and safety.

In this chapter the fundamentals of rocket propulsion will be described, dwelling on hybrid systems. Afterwards there will be a digression about the *Vega* launcher.

1.1 - Rocket propulsion systems

The core of a rocket is the propulsion system, which is the fundamental part useful to accelerate the total mass and insert the payload in a specific orbit. There are multiple different solutions, depending on the energy source and the propellant storage status, each with their own advantages and disadvantages.

1.1.1 – Basic equations

The main target of a rocket [6] is to gain a sufficient ΔV to bring the payload at the requested altitude. The reference law for the evaluation of ΔV in the ideal case (no aerodynamic and gravity forces, no losses) is the Tsiolkovsky equation, which considers the variation of mass of the rocket:

$$\Delta V = I_s * g_0 * ln\frac{m_i}{m_f}$$

where $I_s = \frac{F}{\dot{m} * g_0}$ is the instant specific impulse calculated with average values.

There are 7 fundamental parameters which are the basis of a rocket engine/motor:

- Thrust coefficient $C_F = \frac{F}{p_c * A_t}$ *[F = thrust; p_c = chamber pressure; A_t = nozzle throat area]*
- Characteristic velocity $c^* = \frac{p_c * A_t}{\dot{m}}$
- Effective exhaust velocity $c = c^* * C_F = \frac{F}{\dot{m}}$
- Total impulse $I_t = \int_0^{t_f} F\, dt$ *[t_f = final time of motor function]*
- Specific impulse that can be average ($I_s = \frac{I_t}{m_p * g_0}$) or instant ($I_s = \frac{F}{\dot{m} * g_0} = \frac{c}{g_0}$)
- Mixture ratio $MR = \frac{\dot{m}_O}{\dot{m}_F}$
- Thrust $F = \dot{m} * w_e + A_e * (p_e - p_0)$, where the exhaust velocity at nozzle exit is $w_e = \sqrt{2 * C_p * T_c * \left[1 - \left(\frac{p_e}{p_c}\right)^{\frac{\gamma-1}{\gamma}}\right]}$

1.1.2 – Structure

The main structure of a classic rocket propulsion system [6], that works through the thermo-fluid-dynamic acceleration of propellant exhaust gases, is the thrust chamber, which is the core of the system. It is divided in two parts: the combustion chamber, where the propellant is heated at a high pressure, and the converging-diverging nozzle, where the exhaust gases expanse. If liquid propellant components are present, the structure will also contain a tank and a feed system (ducts, valves, injectors, supply pressure control, etc.). The pressure control system can use two methods to compensate for losses of the feed system.

- Pressurized systems, divided in 3 categories:
  - Regulated tank pressure, where a helium gas tank at a high pressure is connected to the propellant tank. The propellant tank pressure p_t is maintained constant at an optimal value thanks to particular regulation valves.

- Blowdown, where the inert gas (helium) is all contained in the propellant tank at an initial pressure. During operation the tank empties gradually decreasing p_t. This method has the advantage to be simple and light, but with a worst performance.

- Partially regulated, which is a union of the two previous systems. In fact the operation starts with a p_t=cost phase (thanks to the emptying of helium tank), followed by a blowdown phase.

- Turbopump systems, with more costs and mass but the best performance.

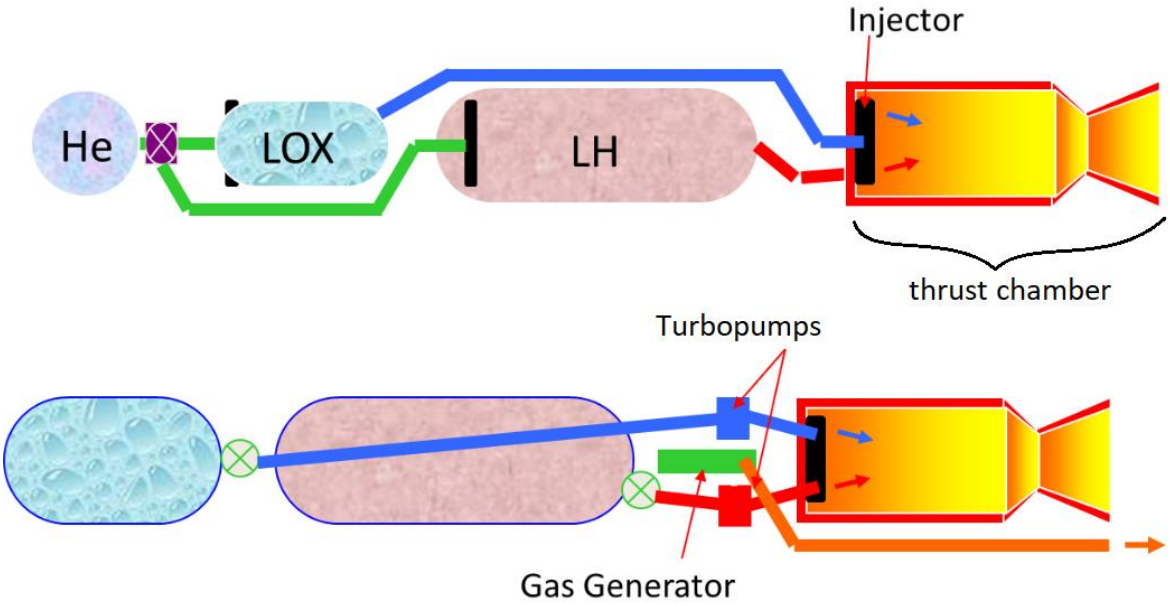

Figure 1: LRE with "pressurized and regulated feed system" (up) and "turbopump system" (down) [8]

1.1.3 – Categories

The main difference [6] between a MOTOR and an ENGINE is that the second has the possibility of adjustments during operation in order to control it (throttle control of thrust). So there are many types of rockets depending on a lot of factors (i.e., type of propellant, source of energy, storage status of the propellant), which can highlight this difference.

The acceleration of the propellant can be of two types:

- Thermo-fluid-dynamic, that can provide a maximum ΔV of the order of 10 km/s, and it works with a fluid (gas) expanded in a nozzle and so accelerated transforming the chemical energy into kinetic energy. To heat the propellant and create the gas, the source of energy can be chemical, nuclear, electric or external (solar or laser).
  There is a limit of ΔV because the value of the effective exhaust velocity is limited to $c = \sqrt{2 * \eta * H_i}$ where H_i is the propellant calorific value and η is the efficiency.

- Electrostatic/Electromagnetic, with a maximum ΔV of 100 km/s, where it's possible to accelerate respectively ions with electric fields or plasma with electromagnetic fields. The energy type is electric, obtained from a nuclear, solar or laser source.

<table>
<tr><th colspan="3">propellant acceleration principle</th><th>energy source</th></tr>
<tr><td rowspan="7">thermo-fluid-dynamic</td><td rowspan="3">chemical</td><td>liquid propellants</td><td rowspan="3">chemical</td></tr>
<tr><td>solid propellants</td></tr>
<tr><td>hybrid propellants</td></tr>
<tr><td rowspan="3">nuclear</td><td>isotope decay</td><td rowspan="3">nuclear</td></tr>
<tr><td>fusion</td></tr>
<tr><td>fission</td></tr>
<tr><td colspan="2">solar-thermal</td><td>solar</td></tr>
<tr><td colspan="2">electro-thermal</td><td rowspan="3">solar/nuclear/laser</td></tr>
<tr><td colspan="3">electrostatic (ions)</td></tr>
<tr><td colspan="3">electromagnetic (plasma)</td></tr>
<tr><td colspan="3">solar sail</td><td>solar</td></tr>
</table>

Table 1: rocket propulsion systems categories [7]

The most common used rockets in history are chemical (chemical energy contained into the propellant), especially through the combustion of the fuel with an oxidizer, which creates an exhaust gas expanded in the nozzle. The subdivision in categories is based on the storage status of the propellant components:

- Liquid rocket engine (LRE) has both the components in the liquid state. It needs the presence of two different tanks and a double feed system, increasing the total mass of the rocket. The main advantage

is the possibility to control the engine and to regulate pressure, increasing the performance.

- Solid rocket motor (SRM) is characterized by the presence of a solid grain contained in the combustion chamber where fuel and oxidizer are already mixed. The main advantage is the mass savings, but on the other hand it's impossible to control or restart the motor, with also the risk of DDT (deflagration to detonation transition), a really dangerous event caused by the presence of cracks on the surface of propellant grain.

- Hybrid rocket motor/engine (HRM/HRE) has characteristics from both the previous systems, in fact the most common combination is made using a solid grain of fuel with a liquid oxidizer. In this case the feed system has only one line coupled with one tank, so the hybrid rocket is simpler than the liquid one. This type of rocket can be throttle controlled (HRE), but the case studied in this work analyses a HRM which doesn't have thrust control but only a partially regulated pressure system of oxidizer tank.

1.2 - Hybrid rocket motors

The necessity of new features [1] including high performance, storability, non-toxicity and safety of rocket propellants made the study of hybrid rockets more important. In fact, restart ability and throttling ability, not reachable by an SRM, are significant, while on the other hand an LRE is complicated and very expensive to develop, although it could be the best solution in term of performance. That's why a hybrid rocket is an excellent compromise, due to positive qualities like simplicity, safety, propellant storability and non-toxicity, stop and restart ability, throttling ability. Moreover, fuel and oxidizer are separated and stored in different phases, increasing the safety level and avoiding significant hazards of manufacturing, shipping and handling SRMs' propellant grains. Typical disadvantages of hybrid rockets are poor regression rate, low combustion efficiency and mixture ratio shifting.

	Advantages over	
Feature	**Liquids**	**Solids**
System	• Mechanically simpler • Less liquids – simpler injection, feed and control systems	• Chemically simpler (including fuel preparation process) • Restartable, throttle able
Safety	• Reduced fire hazard • Less prone to hard starts	• Reduced explosion hazard • Zero TNT equivalent • Able to stop
Performance	• Higher propellant density • Possible to improve performance by the addition of metals	• Higher performance
Environment	• Comparable with RP-1/LOX	• Does not need any toxic and harmful propellant

Table 2: advantages of hybrid propellants over liquid and solid [1]

The choice to implement a hybrid rocket motor for the work [3] concerns the interest to simplify the system not implementing a throttle control (from here the nomenclature "motor"). In fact the only way to throttle a hybrid rocket is controlling the liquid oxidizer mass flow, which has a non-linear correlation with the fuel grain, so the mixture ratio shifting phenomenon arises and the thrust level (non-linearly dependent from MR) suffers for this. Adding an aft-

end injector and a mixer it's possible to control both mixture ratio and the thrust level but complicating and making heavier the system.

1.2.1 – History

Hybrid rockets [4] were performed for the first time in the late 1930s simultaneously in Germany and in California. The first person to theorize hybrid propellant rockets was the German chemical engineer Leonid Andrussow. He tested a 10 kN hybrid rocket motor using solid coal and gaseous N_2O. The *California Pacific Rocket Society* came in the 1940s to use LOX in combination with several different solid fuel types including wood, wax and rubber, concluding with success in 1951 the fly of a LOX/rubber rocket at an altitude of 9 km.

The next studies involved numerous tests with different fuels and oxidizers in order to find the best combination and to analyse the type of combustion. One important discovery regarded the resolution of the big problem of SRM's grains called DDT. In fact the presence of cracks in the fuel grain of a HRM doesn't affect combustion. Also other aspects (positive and negative) of combustion were discovered, like the necessity of a high mixture ratio or the low burning rates (small regression rate of the grain).

In the 1950s a reverse hybrid motor was also studied. In this case the oxidizer was solid and William Avery used jet fuel and NH_4NO_3 using MR = 0.035 only.

In the 1960s, European organizations also started to work on hybrid rockets: the French *ONERA* studied a hypergolic[1] rocket motor (HNO_3/amine) that flew 8 times at the maximum altitude of 100 km, but also the Swedish *Volvo Flygmotor* used a hypergolic propellant combination (HNO_3/polybutadiene with an aromatic amine) to transport a 20 kg payload at 80 km.

The next years (1970-1995) became a continuous succession of new solutions and tests all over the world. Especially in the US many companies started to approach this type of rocket (usually for military applications), reaching excellent performance and beating all records.

After 2000 [5], a lot of commercial companies and universities started to implement this type of technology, considering HRM one of the best solutions

[1] propellant combination whose components spontaneously ignite when they come in contact with each other.

for future space flights. The best example is the company *Scaled Composites*, which designed *SpaceShipOne*, the first private spacecraft, realizing in 2004 the first of three successful manned suborbital (reaching an altitude above the 100 km Karman line[2] without making a complete orbit around the planet) flights with a hybrid motor. The next generation of hybrid private spacecrafts brought to the evolved version *SpaceShipTwo*, produced by the company *Virgin Galactic* from 2007 and tested in 2013. The project expected the use of it for space tourism suborbital flights, with a capacity of 6 passengers and 2 pilots and a ticket cost of $250,000. After initial problems and big failures (2007 and 2014), the *VSS Unity* prototype (evolution of *SpaceShipTwo*) completed in 2018 a powered and manned flight at 83 km.

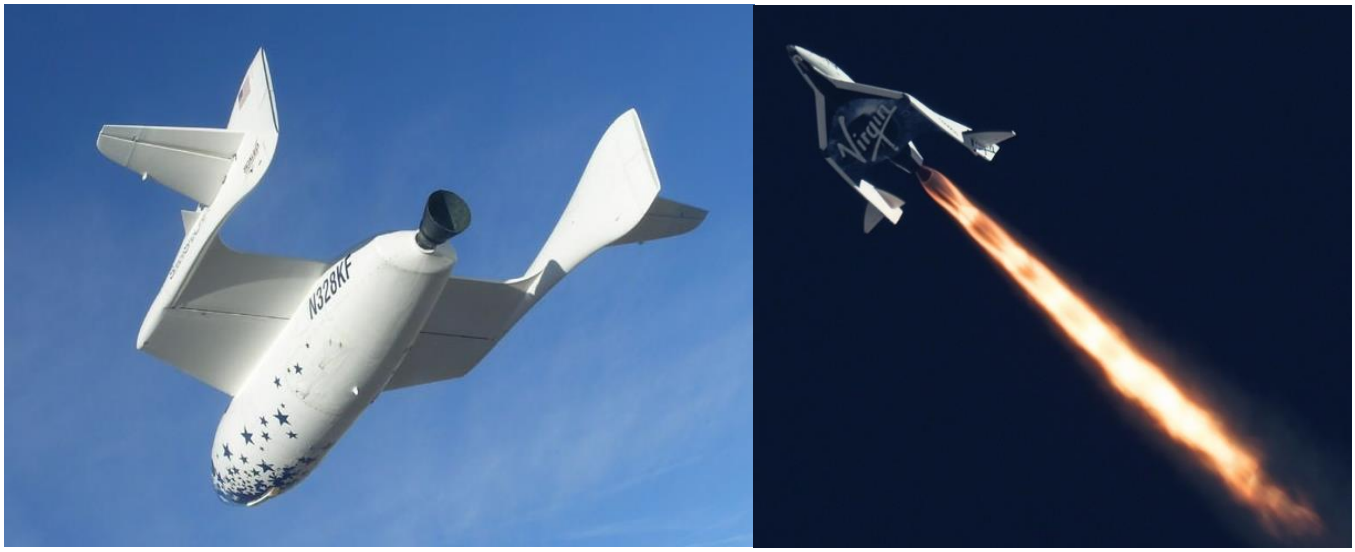

Figure 2: SpaceShipOne (2004) and SpaceShipTwo (2013) [5]

[2] accepted point of entry to space as defined by the International Astronautical Federation.

1.2.2 – Main structure

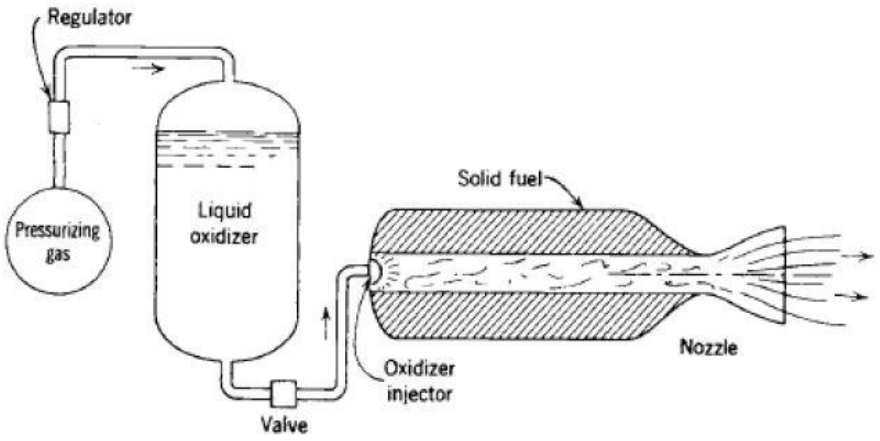

Figure 3: simplified structure of a HRM [6]

The classical characteristic of a HRM [1,6,9] is that propellants are stored in separate phases. The fuel is stored as a grain directly in the combustion chamber. The inner fuel surface, which delimitates the port area, melts and vaporizes due to convection and radiation heat transfer. Liquid oxidizer is injected into the chamber and combustion occurs. The typical oxidizer feed system, represented in *Figure 3*, is pressurized and regulated by the helium gas tank. This method is simpler, lighter and cheaper than a turbopump one, but can be simplified more using a blowdown system, although with a worst performance.

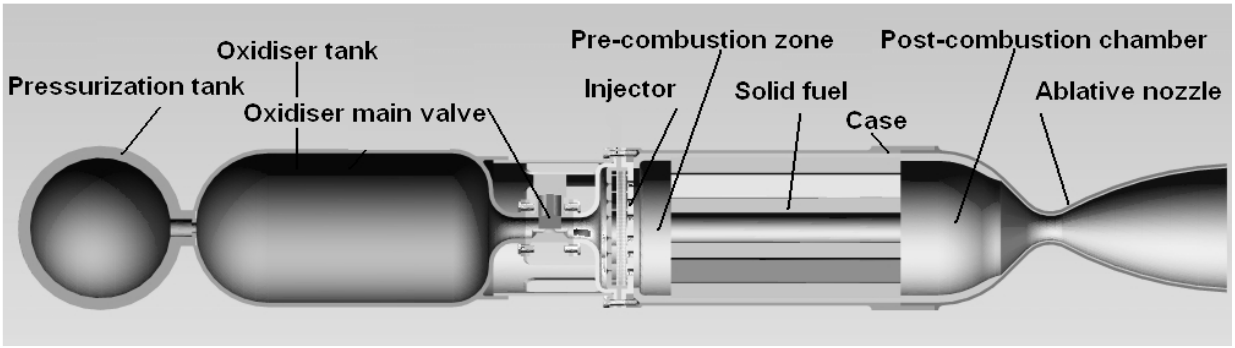

Figure 4: complete scheme of HRM with pressurized and regulated feed system [1]

The more complete scheme in *Figure 4* represents a larger number of components of a HRM. In fact it's possible to individuate two different zones of the combustion chamber. The first before the grain is called "pre-combustion zone" where the oxidizer injected is premixed before burning, the second one is at the end of combustion chamber and it's called "mixer" or

“post-combustion chamber”. The mixer is fundamental for hybrid systems because it’s a remixing zone before the nozzle where the unburned propellant can complete combustion, in fact there is not enough time and space along the grain for a complete burning. The use of mixer can be essential in case of throttle regulation in an HRE. In this case the excess of oxidizer due to regulation is supplied to the mixer with aft-end injectors in order to maintain the global MR always constant. The thrust device is a convergent-divergent nozzle with a thermal protection system composed by an ablative layer.

1.2.3 – Propellants

Typical propellants [1,9] used in HRM are the result of a lot of research. In fact many factors are fundamental: regression rate, type of combustion, calorific value, etc. The only certainty concerns that the best propellant storage status combination is solid for the fuel and liquid for the oxidizer.

The *FUEL* is contained directly in the combustion chamber as a solid grain. It is normally a cylinder with a centred hole fuel port area, which can have particular multi-port geometries in order to increase the burning surface.

The first type of fuels used in history were semi-solid gasoline, wood and coal. Later chemical industry development made possible to use polymers, whose most used are:

- Polyethylene (PE), applied in HRM as “High Density Polyethylene”.
- Poly-Methyl Methacrylate (PMMA, Acrylic or Plexiglas)
- Poly-Vinyl Chloride (PVC)
- Hydroxyl Terminated Poly-Butadiene (HTPB), the most common synthetic rubber with excellent energy and mechanical properties.

Hybrid fuel may contain the addition of metal powder in order to improve performance, in fact the use of magnesium or aluminium (as a fine powder between 2 and 50 μm) affects the regression rate.

Also hydrocarbon family might be also considered for hybrid fuels. The first possibility regards light hydrocarbon mixtures (e.g. petrol), which are normally at liquid phase, but they could be frozen and used as a solid fuel grain, increasing the regression rate. However this solution causes many difficulties in the storage process because light hydrocarbons have a low freezing point.

Therefore the best hydrocarbon is the wax (paraffin based fuels), which is solid even in the ambient temperature simplifying the storage process.

The *OXIDIZER* is instead contained in a tank in the liquid phase, so it's necessary a feed system (usually of the type "pressurized gas" or "blowdown") for supply.

LOX (Liquid Oxygen) is the most commonly used liquid oxidizer because it guarantees high performance, in particular specific impulse. On the other hand it is cryogenic (if preserved at 90K) and it needs a pyrotechnic ignition device, which can be used only once, making the hybrid motor not restart able. An alternative to this problem can be gaseous ignition, complicating the system significantly, and risking, if LOX vaporizes before the mixture forms, the intensification of low-frequency combustion instabilities.

The alternative for LOX is the Nitrous Oxide or Dinitrogen Monoxide (N_2O), also a cryogenic liquid, although it can be stored in liquid phase at the ambient temperature (20°C) but at the pressure of ~60 bar. This is an advantage because it's possible to eliminate additional pressurization devices in the oxidizer feed system. N_2O is the most common oxidizer used for HRMs in history (e.g. it was used for *SpaceShipOne* and *SpaceShipTwo* manned spacecrafts), probably because it's easy to handle and relatively easy to acquire.

There are other common nitrogen compounds used as oxidizers like Nitric Acid (HNO_3) and Nitrogen Tetroxide (N_2O_4).

The highly interesting liquid oxidizer for hybrid application is Hydrogen Peroxide (H_2O_2) [1], which is used as a rocket propellant at 80-98% concentration (called High Test Peroxide). It decomposes both catalytically and thermally in water vapour and O_2 at a decomposition adiabatic temperature between 900 and 1100K. The advantage is the possibility to eliminate additional ignition devices; furthermore H_2O_2 itself as well as its decomposition products are environmentally friendly.

1.2.4 – Combustion theory

The type of combustion of a HRM is particular [1,6], in fact the different storage phases implicate that solid fuel must vaporize and form mixture with the oxidizer in order to ignite and start burning. Combustion, as illustrated in *Figure 5*, is confined in a limited zone within the boundary layer, in fact the flame is small and chemical reactions are quick.

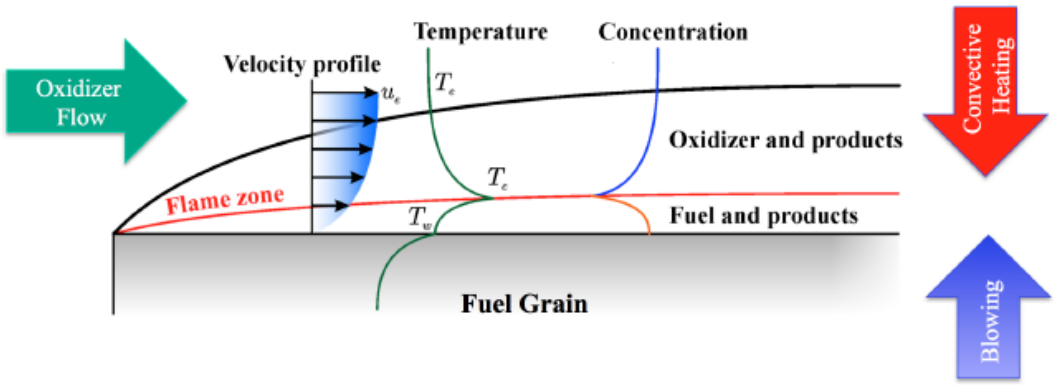

Figure 5: simplified model of the HRM combustion [10]

However two problems could occur:

- The first problem which occurs is the *low-frequency instability*, when the combustion products obstruct the oxidizer inflow limiting mixture formation. Temperature and chamber pressure temporary decrement and then, when combustion restarts normally, they both grow generating high amplitude (even 50% of the chamber pressure) and low frequency oscillations, with the risk to expand into the oxidizer feed system.

- The second inconvenience is the low fuel regression rate of a HRM. The problem depends from the heat flow that moves slowly from hot gas to the fuel surface, due to the slowness of the heat convection mechanism. So the fuel vaporization intensity is small, slowing down the regression rate of 1/10 with respect to SRMs (fuel and oxidizer are premixed).

The behaviour of fuel grain can be described by a mathematical model which can evaluate the hybrid fuel regression law. The most useful equation to

calculate regression rate for engineering evaluations was created by Marxman in 1965, and here it's represented in its simplified version:

$$\dot{y} = r = a\left(\frac{\dot{m}_O}{A_p}\right)^n$$

where $G_{ox} = G = \frac{\dot{m}_O}{A_p}$ is the oxidizer mass flux per unit port area. The ballistic coefficients *a* and *n* are determined from experiments. They depend on the type of propellant composition only in case of pure polymer fuels, while, in case of metal addition, also p_c (chamber pressure) influences them.

Propellants	*a*	*n*
HP/PE	7.00E – 06	0.800
HP90%/HTPB	2.47E – 05	0.666
LOX/HTPB	9.29E – 06	0.852
LOX/wax	9.10E – 05	0.690

Table 3: ballistic coefficients for typical propellant combinations (r is m/s; G_{ox} is kg/m²/s) [3]

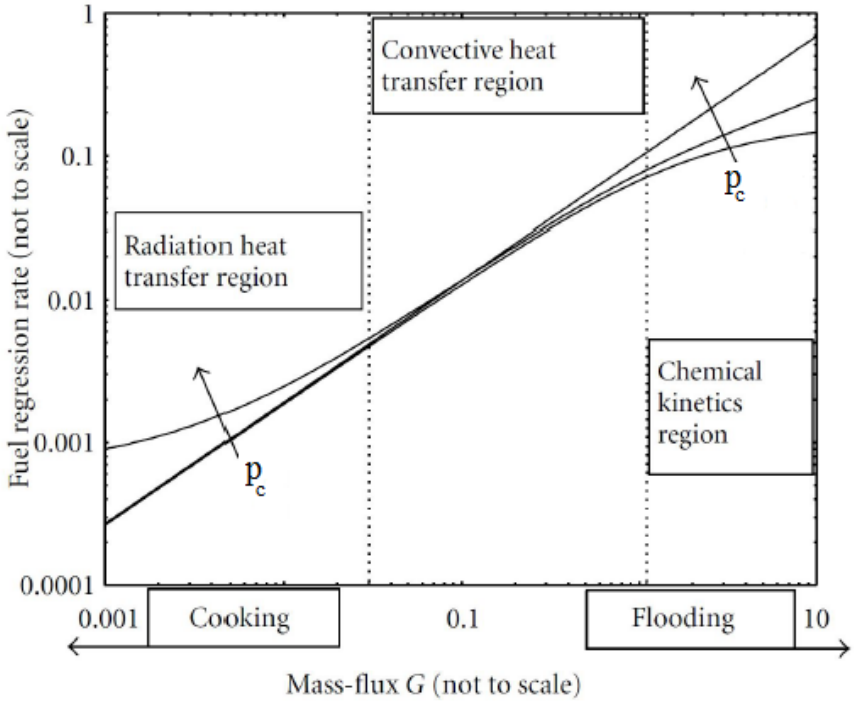

Figure 6: behaviour of regression rate with respect to G_{ox} [6]

The figure above (*Figure 6*) demonstrates how regression rate really varies with respect to G_{ox}. It's possible to locate three regions depending on the value of G_{ox} where the heat transfer from the flame to the grain is controlled by different factors.

- Low values of G_{ox}: the radiation heat transfer is not negligible and the grain tend to melt in the lower layers (cooking). The influence of p_c is relevant.

- Intermediate values of G_{ox}: the main phenomenon which limit the magnitude of *r* is the convective heat transfer. This is the zone where the approximation of $r = a\left(\frac{\dot{m}_O}{A_p}\right)^n$ is considered correct, in fact there isn't dependence from p_c. For the thesis work the choice is to consider relevant only convective heat transfer and valid the regression rate equation.

- High values of G_{ox}: the chemical kinetics controls heat exchanges, so *r* is influenced by p_c. The risk is to extinguish the flame (flooding).

In order to increase the regression rate and mitigate the typical problem of HRMs there are some solutions. It is possible by increasing the fuel surface area (A_b), for example shaping the internal port section (but removing fuel) or using directly multi-port fuel grains (with three main disadvantages: complicated fuel preparation, difficult oxidizer distribution into every port, poor fuel grain integrity. Other solutions regard the addition of small metal particles (magnesium, aluminium) because they absorb more radiation heat from the hot gas but making the burning rate pressure dependent.

Another discovery is the *Liquid Layer Hybrid Combustion Theory* (*Stanford University* 1997) which is applied to hydrocarbon fuels, especially paraffin (wax), for their low melting temperature. During combustion the fuel melts and creates a liquid film on the surface, so single droplets separate from the liquid film and vaporize. Experiments demonstrate that the low melting temperature of hydrocarbons gives an increase of the regression rate.

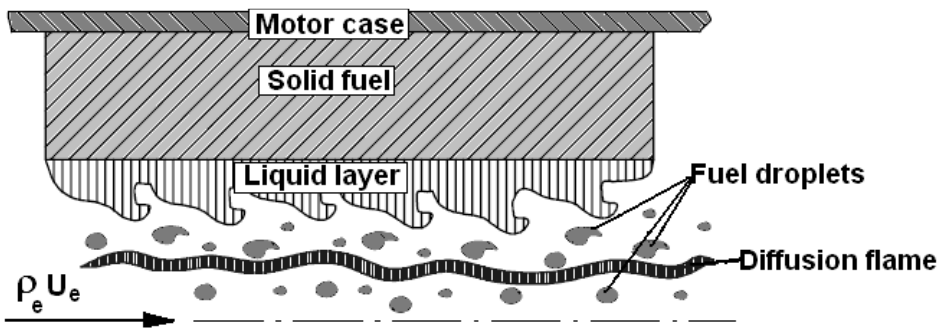

Figure 7: "Liquid layer hybrid combustion theory" for hydrocarbon fuels [1]

Another important aspect regards the problem of *mixture ratio shifting*. In fact HRMs have the inconvenience that MR varies during combustion, precisely because of the fuel grain geometry variation during regression. All this is independent from other motor phenomena which can variate $\dot{m}_O$ (throat erosion, p_c variation, blowdown, etc.) and so MR. The MR shifting of combustion can be demonstrated with simple equations.

$$\dot{m}_F = \rho_b * A_b * r = \rho_b * A_b * a\left(\frac{\dot{m}_O}{A_p}\right)^n = k * \frac{A_b}{{A_p}^n} * {\dot{m}_O}^n$$

so, considering $\dot{m}_O$=cost, in order to maintain MR=cost it's necessary that

$$\frac{A_b}{{A_p}^n} = \frac{2 * \pi * R * L}{\pi^n * R^{2n}} = cost$$

and it is possible only if *n* = 0.5 (radial fuel grain), but also with a progressive decrease of *r*. The typical situation is characterized by *n* > 0.5, so in this case MR will increase during combustion.

Another fundamental aspect to take into consideration is the possibility of throttle adjustment, which is typical of a hybrid rocket engine. The only way to regulate a hybrid system is the control of the oxidizer mass flow. Changing the value of $\dot{m}_O$, two main parameters are affected at the same time:

$$\dot{m}_F = k * \frac{A_b}{{A_p}^n} * {\dot{m}_O}^n$$

$$MR = \frac{\dot{m}_O}{\dot{m}_F} = \frac{{\dot{m}_O}^{1-n}}{k} * {A_p}^n * \frac{1}{A_b}$$

So the consequence is that to change fuel flow, which varies slower than oxidizer flow, the MR is automatically modified. In order to maintain global MR=cost, it's necessary to send the excess of oxidizer to the mixer with aft-end injectors. The main inconvenience is that this type of regulation system of a HRE is heavy and expensive with respect to a simpler HRM. So for the thesis work the HRM implemented won't have a throttle regulation system.

1.3 - *Vega* launcher

Vega [14,15] (Italian acronym for "*Vettore Europeo di Generazione Avanzata*" and meaning "*Advanced generation European carrier rocket*"), is an expendable[3] launch system in use by *Arianespace* jointly developed by the *Italian Space Agency (ASI)* and the *European Space Agency (ESA)*. Its development started in 1998 and the first launch took place from the *Centre Spatial Guyanais* in 2012.

Figure 8: Vega [11]

It belongs to small launchers' family (payloads up to 2000 kg in LEO), and it inserts satellites, for scientific and Earth observation missions, mainly into polar[4] LEOs. In its reference mission, *Vega* brings a payload of 1500 kg (with possibility of multiple payloads) to a 700 km polar orbit.

The rocket is a single-body launcher, without strap-on boosters, with three solid rocket stages and a liquid rocket upper module called AVUM. Italy, with the manufacturer *Avio*, is the leading contributor to the Vega program, followed by other European countries.

1.3.1 – Structure

Vega has a total lift-off mass of 137 tons, with a height of 30 m and a maximum diameter of 3 m. It's divided into 4 stages, which control every part of the mission. The payload is contained in a fairing, on the top of the rocket, designed and manufactured by the Swiss company *RUAG Space*. It is made of two composite half-shells, with a diameter of 2.6 m and a length of 7.88 m.

The 4 stages are described below:

- *P80* is [12,17,18] the first SRM stage, which includes a thrust vector control (TVC) system (two electromechanical actuators that operate

[3] launch vehicle that can be launched only once, after which its components are destroyed during re-entry or discarded in space [16].
[4] inclination = 90°

a movable nozzle powered by lithium ion batteries) and a case of 3 m diameter. The solid propellant is HTPB-1912 (aluminium powder 19%, HTPB 12%, oxidizer ammonium perchlorate 69%), a single-piece grain of 88 tons mass. The average thrust is ~2200 kN.

- *Zefiro 23* is [12,18] the second SRM stage, with a carbon-epoxy case (1.9 m diameter) and a carbon phenolic nozzle (carbon-carbon throat insert). The propellant used is HTPB-1912, with a grain mass of 24 tons, giving an average thrust of 871 kN.

- *Zefiro 9* is [12] the third SRM stage, and it's identical to the second stage except for length (3.5 m), mass and performance. In fact it contains 10.5 tons of HTPB-1912 and provides an average thrust of 260 kN.

- *AVUM* (*Attitude & Vernier Upper Module*) is [11,12,13] the *Vega*'s LRE upper-stage (fourth stage). It contains two different propulsion systems:

  - the main propulsion system *RD-843* is useful to place the payload at the required orbit. It's a LRE with a liquid bipropellant combination (fuel is UDMH or unsymmetrical dimethylhydrazine, oxidizer is NTO or N_2O_4 or nitrogen tetroxide) and a pressurized and regulated feed system. It is designed to inject different payloads into different orbits, thanks to its reignitable capacity (up to 5 restarts). The propellant mass is 577 kg and the average thrust during operation is 2.42 kN.

  - the monopropellant propulsion system is necessary to perform roll and attitude control functions. It is possible thanks to two sets of three monopropellant thrusters supplied by 38.6 kg of hydrazine (N_2H_4).

  The two propulsion systems are contained in the *AVUM Propulsion Module* (*APM*). There is also a further module, the *AVUM Avionics Module* (*AAM*), which contains the main components of the avionics sub-system of the vehicle.

Figure 9: Vega subdivision in 4 stages + fairing [13]

1.3.2 – Mission

The *Centre Spatial Guyanais* (*CSG*) [12], based in the French Guyana town of Kourou, offers ideal conditions for launchers. Located at 5° North latitude, its proximity to the equator allows extra acceleration energy due to the Earth's rotation. *Vega* has the advantage to be able to use this excellent European site, in particular the launch pad *Ensemble de Lancement Vega* (*ELV*). Every launch costs 37 million US dollars with a rate of 3-4 launches per year.

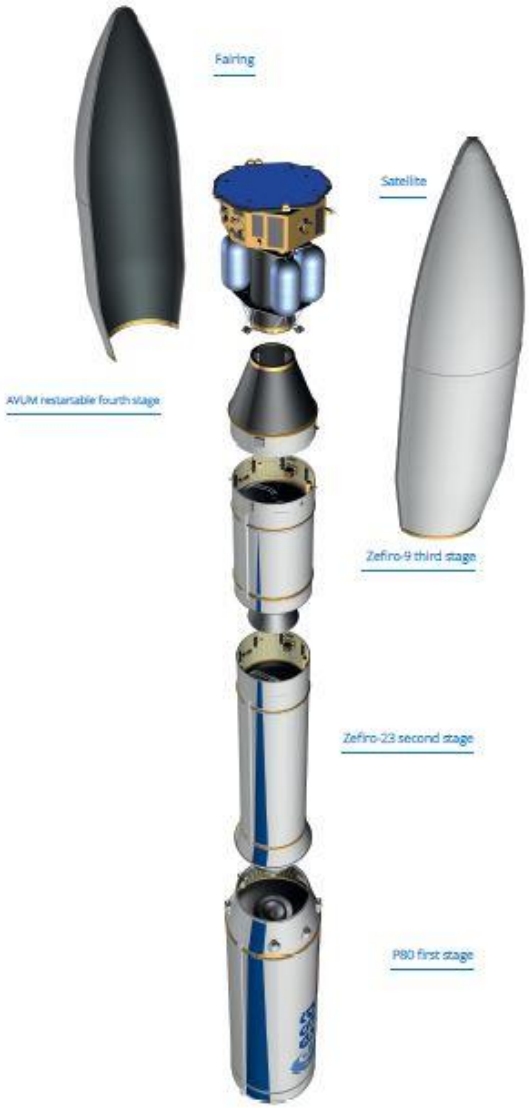

Figure 10: Vega exploded view [12]

With the reference payload capacity of 1500 kg into low Earth orbit (LEO), *Vega* is designed for the launch of small Earth observation, meteorological and scientific satellites delivering them directly into sun synchronous orbits (SSO), polar circular orbits, or circular orbits of different inclinations. This extensive operational flexibility for a wide range of missions is guaranteed by the position of the *CSG* combined with the adaptability of the upper-stage *AVUM*. In fact it has a restart able capacity, with up to 5 burns in flight, permitting to perform the separation of multiple payloads all contained in the *VESPA* (*VEga Secondary Payload Adapter*), a device inside the fairing.

In the figure below (*Figure 11*) it's possible to observe the complete reference mission of *Vega*, with all the steps of every stage ignition and separation.

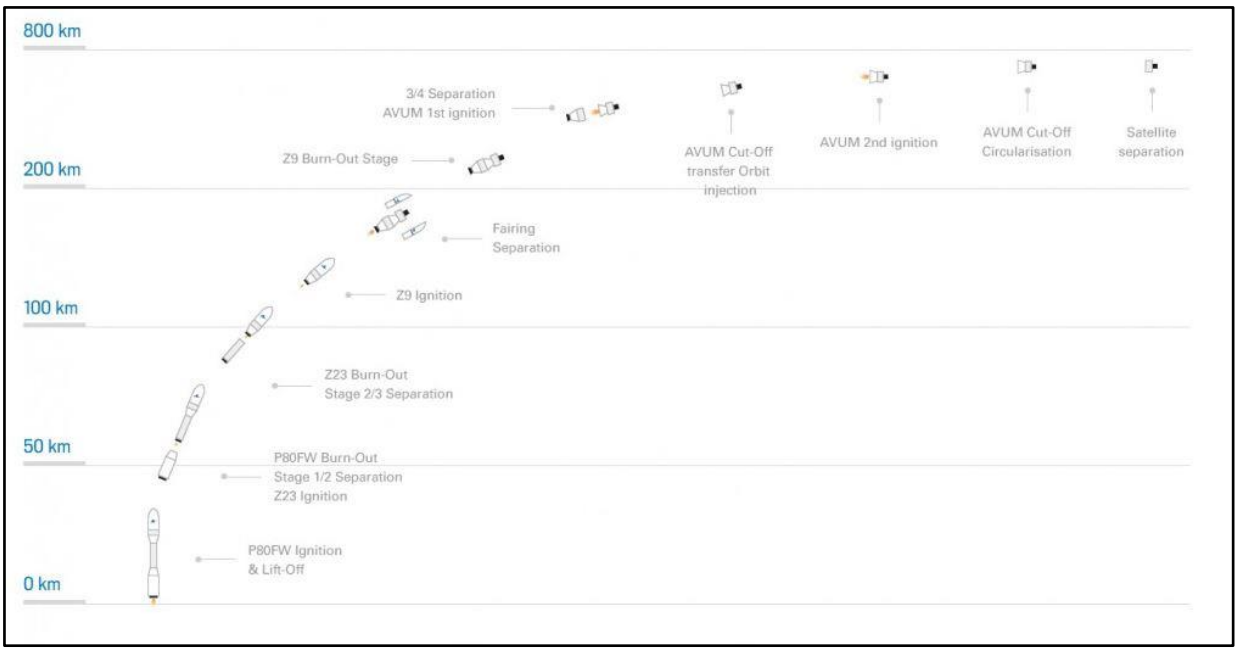

Figure 11: typical complete mission of Vega [12]

As the only launcher in this class now in regular production, *Vega* has become a global benchmark. Its main objective is to provide Europe with a safe, reliable, competitive, and efficient ability to insert payloads in LEO for research or commercial issues. In fact the actual commercial market's requirements need a new generation of lightweight launch vehicles capable of orbiting small to medium-sized satellites.

With 15 successful flights since its introduction in 2012, *Vega* launcher became competitive on the market. After the first and only failure of July 2019, the next and last successful flight so far took place on 3 September 2020.

Figure 12: Vega during lift-off on 3 September 2020 [12]

Chapter 2

Preliminary work

The target of the work is to apply a HRM at the upper-stage of the Vega, studying its behaviour and optimizing motor parameters. That's why it's necessary a preliminary work to describe the modified upper-stage and to understand all the instruments provided for the final analysis. So, the first part of the chapter is dedicated to the description of this new upper-stage, while the second part deals with the *Fortran* code. This code, developed by *Politecnico di Torino*, uses an indirect approach to simulate the trajectory (conditions found to cancel the error) and a direct method for the motor design (payload gradient is cleared with respect to motor parameters).

2.1 – *Vega*'s upper-stage with HRM

The main target of the thesis work is the application of a hybrid rocket motor on the *Vega*'s upper-stage. The modification realized concerns the substitution of the last two stages (3rd with SRM and 4th with LRE) with a unique upper-stage (the last and 3rd stage) equipped with a HRM with partially regulated feed system.

2.1.1 – Mission phases

The mission of the modified *Vega* is similar to a typical original one. The main difference is that the upper-stage has an imposed initial thrust of 50 kN, so the payload value will be lesser than the reference *Vega* one, changing all the rocket sizing and decreasing components' masses. The final orbit, in which the HRM inserts the payload, is a circular orbit with inclination 97.5° at an altitude of 500 km. The phases of the first two SRM stages (*P80* and *Z23*) are considered the same of the original *Vega* launcher and fixed, as reported in the table below.

No.	Phase	Stage
1	Vertical ascent	1
2	Rotation phase	1
3	Ascent	1
4	Coast after first-stage jettisoning	— —
5	Ascent	2
6	Coast after second-stage jettisoning	— —

Table 4: 1st and 2nd stages phases [3]

The 1st stage (*P80*) ignites and, after the lift-off, allows a vertical ascent which becomes inclined through use of the thrust vector control. The jettisoning of 1st stage (separation 1/2) is followed by a coast arc phase. The following ignition of 2nd stage (*Zefiro 23*) permits a further ascent followed by the coast arc after jettisoning (separation 2/3). The fairing phase, where the two half-shells of the fairing separate revealing the payload, is normally realized during the upper-stage burning, but in this case it's concluded before the 2nd stage burn-out, simplifying following calculations. The sizing of these two stages is not contained in this work and the simulation starts from the ignition of the HRM upper-stage (3rd stage) with imposed conditions, in particular at an altitude of 245.75 km and with an initial velocity of 4.57 km/s.

The upper-stage is characterized by a hybrid rocket motor with a partially regulated pressure feed system and without a throttle control. There are different phases of the burning:

- p_t=cost phase, where the pressurized feed system is supplied by two helium tanks which maintain constant the oxidizer tank pressure to an initial value (obtained from motor optimization).
- first blowdown phase; when the pressurizing effect of the helium tanks ends, the oxidizer flow is maintained in blowdown albeit with a loss of performance.
- coast arc phase, with the HRM cut-off leaving a bit of propellant for a second short ignition. During this long phase with motor off the altitude increases thanks to the ΔV previously impressed, it's made the transfer orbit injection.
- last blowdown phase, where, with a reignition using the residual propellant, the injection of the payload at the final orbit is concluded.
- payload separation and deorbit of the upper-stage. The deorbit is possible using a residual propellant margin of 2%.

So the HRM is designed to perform the injection into the final orbit with two burns, making the reignition an important issue for the HRM. Although it is not considered in the present work, the possibility of multi-payload missions, now a typical requirement for *Vega*, shouldn't affect performance using this solution with HRM, due to the small duration and low acceleration needed during the second blowdown burn for the final orbit injection [3].

2.1.2 – Specifications of the upper-stage

The structure of the HRM is characterized by different sections which compose the total system. Some physical quantities are fixed at an initial optimum value, while the motor parameters can be modified to optimize the payload.

The main components of the feed system are the pressurized *HELIUM GAS TANKS*. There are two cylindrical tanks made with composite material and with a fixed radius due to a geometric constraint of space. They are also internally covered with an aluminium liner of 6 mm thickness for safety reasons. The initial pressure of the helium gas is p_{si} = 310 bar, and the pressure losses due to the connection with oxidizer tanks are *dps* = 20 bar.

The *OXIDIZER TANKS* are 4, cylindrical and made with composite material. The radius is the same of the helium gas tanks, and also in this case there is a 6 mm thickness aluminium liner. The initial internal pressure p_{ti} is a motor parameter to be optimized, and the pressure losses due to the connection with combustion chamber are *dpi* = 15 bar.

The HRM is structured so that the 4 oxidizer and 2 helium tanks are arranged laterally to surround the combustion chamber. The total diameter of the stage is imposed to be 1.9 m (*Vega* requirement), and it's respected thanks to the tanks' radius geometric constraint.

The *COMBUSTION CHAMBER* is the core of HRM. Here the combustion occurs between the solid fuel grain and the liquid oxidizer. The choice of propellant combination is made to have a particular value of ballistic coefficients *a* and *n* (*a* = 1.5E-4; *n* = 0.5), so it's considered paraffin (wax) as solid fuel grain and H_2O_2 (hydrogen peroxide) as liquid oxidizer. The wax has the advantage to be a solid hydrocarbon, which particular combustion (formation of liquid layer) permits an increase of the regression rate. All the propellant has a reserve not used for the main mission, but however useful. In fact there is, both for fuel and oxidizer, a double margin: 2% for deorbit of HRM after payload insertion and 5% for safety. The fuel grain is cylindrical, with a single internal cylindrical port, and its dimensions are given in input as tentative values, later corrected with iterations of the code. The cylindrical combustion chamber is made with aluminium and has an internal insulating layer of 12 mm thickness. It is also

present a mixer at the end of the chamber (length 0.5 m) useful to have enough space to complete combustion before exhaust gases nozzle expansion. The chamber pressure (also called “chamber nozzle-stagnation pressure”) is imposed to be at the initial value of $p_{ci} = p_{ti} - dpi$, considering feed system pressure losses. This evaluation of p_c, which varies also with p_t during combustion, is usually sufficient to guarantee that $p_t/p_c > 1.5$ in order to avoid coupling between the hybrid motor and the oxidizer feed system and so the possibility of low-frequency instability [3].

The second part of the thrust chamber is the *NOZZLE*. It is converging-diverging with angle 45°-15° and made with aluminium. The internal coverage is composed by an ablative layer for thermal protection, which thickness is maximum at the throat. The typical phenomenon which occurs is the throat erosion of the ablative layer, that influences parameters (e.g. p_c, ε, J) and performance.

The total upper-stage is very compact in size, due to the arrangement of the tanks around the combustion chamber. The total length of the motor that matters is the sum of combustion chamber and nozzle length (thrust chamber). All the rocket stage is finally contained in an aluminium *CASE* with 30 mm thickness for protection. The length-to-diameter ratio *L/d*, in comparison with the typical values for LREs, can be used as an index of marketability of the HRM. In fact the existing infrastructures projected for LRE can be reused for this new solution, and in addition, a small *L/d* permits low vehicle loads [3].

2.2 – *Fortran* code comprehension

The code is composed by 3 fundamental parts:

- *o42.for* that is the main code
- *p2hpwaxheero.for* with a lot of subroutines
- *t2vhpwaxero.for* with subroutines about various aspects including masses evaluation and output values writing

Also other code parts of the type *".for"* are included in the work and they are fundamental for a correct compilation. To compile the code it was used a program called *f90* which can run only on a Virtual Machine with *Windows XP* software. The result is an executable code called *o42.exe* which can be run from a command window. To run the code are necessary some files including *STATM.DAT* (for Standard Atmosphere evaluation), *input.txt* (with input values from which to start the optimization) and *ASC2V.DAT* (with other important input values for the simulation, in particular the unknown initial values). All the values given in input are tentative, which can be corrected by the simulation.

The code launch starts with the request in input of two values: r_{min} e *pbis*. The r_{min} number decides the behaviour of iterations. In fact if it is equal to 0 the code completes only one iteration, modifying input try values but without correcting them for the optimization, if otherwise it's greater than 0 the number value decides the precision of correction during iterations. In fact to have a better result it's necessary to impose a small value of r_{min} (typically 0.1) but increasing a lot the number of iterations. The value of *pbis*, which represents how much the error is admitted at each iteration, is instead fixed at 2.

When the code ends, it writes on the command window the main output results and asks a request: "to print the values on disc?". Answering "yes" all the try numbers contained in *input.txt* and *ASC2V.DAT* are overwritten with the new ones found after the code running.

2.2.1 – Description of *input.txt* file

The fundamental tool for the simulation is the *input.txt* file. It provides to the code the 6 fundamental parameters from which to start the simulation,

adding also two values related to the type of propellant, here fixed (a = 1.5E-4; n = 0.5).

In the *input.txt* file also other try values are contained, but they are calculated automatically and overwritten after running the code. Below an example of input file, containing reference values, is represented.

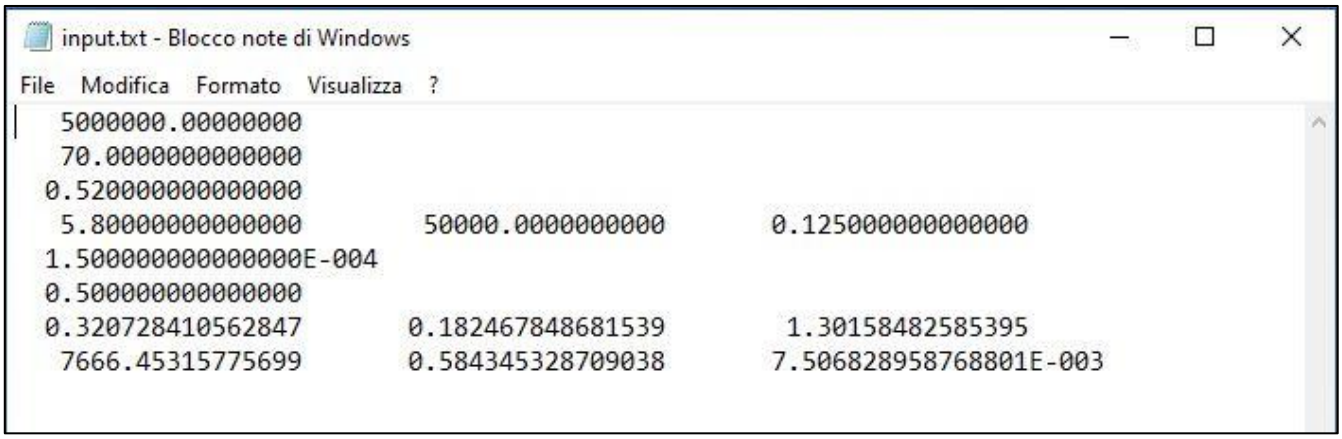

Figure 13: input.txt file with nominal case values

These are the values contained in order in the *input.txt* file:

pt_i [bar]		
eps		
amo1		
MR_i	**thrust_i** [kN]	**J = (At/Ap)i**
a		
n		
grain ext radius [m]	**web** [m]	**grain length** [m]
R_idr [Pa*s/m^3]	**amof**	**At iniz** [m^2]

Table 5: input.txt file values description

- *amo1* = oxidizer mass fraction consumed during the phase p_t=cost ($m_{O\_pt=cost}/m_{iniz}$)
- *amof* = total oxidizer mass fraction consumed (m_O/m_{iniz})
- *grain ext radius* = external radius of the fuel grain (without reserve)
- *web* = web thickness of the grain
- *eps* = initial ε value (A_{ex}/A_{ti}) -> throat erosion decreases ε

2.2.2 – Code calculation method

The *Fortran* code used for the work [3] realizes a coupled optimization of motor design and trajectory. To deal with motor design parameters a direct method is employed, while, for each choice of the motor parameters, an indirect method is chosen to optimize the trajectory. This type of approach derives from the different characteristics of motor design and trajectory.

An indirect approach is perfect for trajectory optimization, normally characterized by continuous controls (e.g. thrust direction, motor burning times), because it is quite accurate and doesn't require a large number of parameters. It works with the goal to find certain optimal conditions in order to cancel errors. The main constraint is that the indirect method requires relations written explicitly (as differential equations), so it cannot be used to determine the motor behaviour.

The motor model requires maximum 4 design parameters to be optimized, so a direct method can be employed. In this case the payload gradient is cleared with respect to motor parameters. However, for being a local optimization method, it requires an initial tentative solution, which influences the result of the optimization procedure, risking getting stuck on a local optimum.

The **trajectory model** considers a point mass rocket, which behaviour is described by the state equations, providing the time derivative (variation) of position *r* (radius, latitude and longitude), velocity *v* (three components), and rocket mass *M*. The equations are reported below:

$$\dot{\boldsymbol{r}} = \boldsymbol{v} \qquad \dot{\boldsymbol{v}} = \boldsymbol{g} + \frac{\boldsymbol{F} - \boldsymbol{D}}{M} \qquad \dot{M} = -\frac{|\boldsymbol{F}|}{c^* C_F}$$

The effect of forces is taken into account considering an inverse-square gravity field, calculating the aerodynamic drag $D = 0.5 * \rho_{amb} * C_D * S * v_{rel}^2$ and evaluating thrust $F = F_{vac} - \varepsilon * A_t * p_{amb}$. The trajectory is split into the phases outlined in section 2.1.1.

The **motor design and operation model** (with a direct method) is accessed many times by the optimization procedure. This model, which contains a lot of

equations, must be simple in order to be fast and reliable for the optimization. The main equations necessary to evaluate important **motor design** values are illustrated below. The evaluation of thrust coefficient depends on altitude, ε and p_c.

$$C_F = 0.98 * \left\{ \sqrt{\frac{2*\gamma^2}{\gamma-1} * \left(\frac{2}{\gamma+1}\right)^{\frac{\gamma+1}{\gamma-1}} * \left[1 - \left(\frac{p_e}{p_c}\right)^{\frac{\gamma-1}{\gamma}}\right]} + \varepsilon * \frac{p_e}{p_c} \right\} - \varepsilon * \frac{p_{amb}}{p_c}$$

Now it's possible to calculate initial values for each quantity finding the propellant mass flow and so the grain and nozzle geometry, as described below.

$$\left(\dot{m}_p\right)_i = (1+\alpha_i)(\dot{m}_F)_i = \frac{1+\alpha_i}{\alpha_i}(\dot{m}_O)_i = \frac{F_i}{c_i^* * C_{Fi}}$$

$$A_{ti} = \frac{(\dot{m}_p)_i * c_i^*}{p_{ci}}; \qquad A_{pi} = \frac{A_{ti}}{J_i}; \qquad A_{bi} = \frac{(\dot{m}_F)_i}{\dot{y}_i * \rho_F}$$

$$\dot{y} = a\left(\frac{\dot{m}_O}{A_p}\right)^n$$

During **operation** it's possible to evaluate the motor performance, especially p_t that is constant for the first phase and then decreases during the blowdown phase, assuming an isentropic expansion of the pressurizing gas while the oxidizer volume in the tank decreases (leaving more volume for the gas).

$$p_t = p_{ti} * \left(\frac{V_{gtBD}}{V_{gt}}\right)^{\gamma}$$

The following system of five nonlinear equations is solved numerically at each time instant, given the tank pressure and the motor geometry obtained previously.

i. $p_1 = \left[1 + 0.2 * \left(\frac{A_t}{A_p}\right)^2\right] * p_c$

[Along the combustion chamber there are pressure losses between the head-end and the nozzle-stagnation zone. So the chamber head-end pressure p_1 is a function of the chamber nozzle-stagnation pressure p_c.]

ii. $\dot{m}_O = \sqrt{(p_t - p_1)/R_{idr}}$
[Considering an incompressible turbulent flow, where R_{idr} = hydraulic resistance]

iii. $\dot{m}_F = \rho_F * \dot{y} * A_b$

iv. $MR = \frac{\dot{m}_O}{\dot{m}_F}$

v. $p_c = \frac{(\dot{m}_O + \dot{m}_F) * c^*}{A_t}$

To integrate the trajectory equations, it's necessary also to calculate the thrust level $F = p_c * A_t * C_F$, determined by evaluating C_F at the actual altitude.

The overall propellant is finally evaluated at burnout and an estimation of the structural masses can be obtained to size the motor at the end of the simulation. All the necessary steps are illustrated in the next section 2.2.3.

2.2.3 – Masses evaluation

The code *t2vhpwaxero.for* contains an important section dedicated to masses evaluation. Here all the parts of the motor are analysed calculating the mass of every single component. This is the core of the simulation because the final result is the payload, which is the fundamental value to be optimized.

Below all the code section will be reported with comments in squared brackets.

```
zprop = min * (1 - dmf - y(7))        [z = m = mass; dmf = fairing mass fraction = 0;
                                       y(7) = upper-stage final mass fraction]

Ri = (Api / π)^0.5                    [Ri = initial internal grain radius; Api = initial port area]
```

$web_{tot} = 1.07 * web$ *[web = web thickness]*

$R_{ex\_tot} = R_i + web_{tot}$ *[cylindrical grain external radius with reserve]*

$A_{Fi} = \pi * R_{ex\_tot}^2 - A_{pi}$ *[initial grain cross section with reserve]*

$z_{Ftot} = A_{Fi} * L_F * \rho_b$ *[□F = fuel grain; LF = grain length; ρb = fuel density]*

$A_{pf} = \pi * (R_i + web)^2$ *[final port area]*

$A_{Ff} = \pi * R_{ex\_tot}^2 - A_{pf}$ *[final grain cross section (fuel reserve)]*

$z_{F\_res} = A_{Ff} * \rho_b * L_F$

$z_F = z_{Ftot} - z_{F\_res}$

$z_O = z_{prop} - z_F$

$z_{Otot} = 1.07 * z_O$

$z_{O\_res} = z_{Otot} - z_O$

$V_{tank} = z_{Otot} / \rho_O + V_{gi}$ *[□tank = ox. tank; ρO = ox. density; Vgi = initial helium gas volume in ox. tank (ullage)]*

$D_{grain} = 2 * R_{ex\_tot}$

$s_{cc} = p_{ci} * R_{ex\_tot} / \sigma_{al}$

[s_{cc} = aluminium combustion chamber thickness; p_{ci} = initial chamber pressure; σ_{al} = aluminium yield stress]

$R_{cc} = R_{ex\_tot} + 0.013$

$D_{cc} = 2 * R_{cc}$

$L_{cc} = L_F + 0.5$

[L_{cc} = grain length + mixer, mixing zone for a complete combustion]

$z_{cc} = \pi * (L_{cc} * 2 * R_{cc} * s_{cc} * \rho_{al} + L_F * (R_{cc}^2 - (R_{cc} - 0.012)^2 * \rho_{vr})$

[the grain is laterally covered by an insulating layer with thickness = 0.012 m and density ρ_{vr}]

$V_{se} = (amo1 * m_{in} / \rho_O) * p_{ti} / (p_{si} - p_{ti} - dps)$

[□$_{se}$ = helium gas tank; amo1 = ox. mass fraction consumed during the phase p_t=cost; p_{si} = helium gas tank initial pressure; p_{ti} = ox. tank initial pressure; dps = pressure losses]

$z_{gas} = (p_{ti} * V_{gi} + p_{si} * V_{se}) / R_{gas} / T_{gas}$

$R_{se} = (0.9 - (R_{cc} + s_{cc}))/2$

$L_{se} = V_{se} / 2 / \pi / R_{se}^2$ *[there are 2 composite cylindrical helium gas tanks]*

$D_{se} = 2 * R_{se}$

$s_{se} = p_{si} * R_{se} / \sigma_{comp}$

$R_{ss} = R_{se} + s_{liner}$ *[there is an internal aluminium liner for safety]*

$z_{se} = 2 * (\rho_{comp} * 2 * \pi * (R_{ss} * L_{se} * s_{se} + R_{ss}^2 * s_{se}) + \rho_{al} * 2 * \pi * (R_{se} * L_{se} * s_{liner} + R_{se}^2 * s_{liner}))$

$p_{sef} = p_{ti} + dps$

$T_{sef} = T_{gas}$

$z_{gsi} = p_{si} * V_{se} / R_{gas} / T_{gas}$ *[initial helium gas mass in the full gas tank]*

$z_{gsf} = p_{sef} * V_{se} / R_{gas} / T_{sef}$ *[final helium gas mass in gas tank]*

[helium gas mass, volume and temperature in the ox. tank at the end of p_t=cost phase; pressure = p_{ti}]:

$z_{gt} = z_{gas} - z_{gsf}$

$V_{gti} = V_{gi} + amo1 * m_{in} / \rho_O$

$T_{gti} = p_{ti} * V_{gti} / z_{gt} / R_{gas}$

[helium gas volume, pressure and temperature in the ox. tank at the end of blowdown phase; mass = z_{gt}]:

$V_{gtf} = V_{gi} + z_O / \rho_O$

$p_{gtf} = p_{ti} * (V_{gti} / V_{gtf})^{\gamma}$

$T_{gtf} = p_{gtf} * V_{gtf} / z_{gt} / R_{gas}$

$R_t = (A_{ti} / \pi)^{0.5}$ *[R_t = nozzle throat radius; A_{ti} = initial throat area]*

$D_t = 2 * R_t$

$R_{ex} = R_t * (eps)^{0.5}$

$R_{tank} = (0.9 - (R_{cc} + s_{cc}))/2$

$L_{tank} = V_{tank} / 4 / \pi / R_{tank}^2$ *[there are 4 composite cylindrical oxidizer tanks]*

$D_{tank} = 2 * Rt_{ank}$

$s_{tank} = p_{ti} * R_{tank} / \sigma_{comp}$

$R_{ts} = R_{tank} + s_{liner}$ *[there is an internal aluminium liner for safety]*

$z_{tank} = 4 * (\rho_{comp} * 2 * \pi * (R_{ts} * L_{tank} * s_{tank} + R_{ts}^2 * s_{tank}) + \rho_{al} * 2 * \pi * (R_{tank} * L_{tank} * s_{liner} + R_{tank}^2 * s_{liner}))$

$time = ((tbf + yp(1) + yp(2) + yp(4)) * t_{conv})$ *[time = total time of propellant combustion]*

$$port = z_{prop} / time$$ *[port = average propellant flow during all combustion]*

$$coef = \exp(-(10/0.7) * (2 * R_t)^{1.8} / port^{0.8})$$

$$s_{abl} = 0.000787 * time^{0.68} * coef + y(16)$$ *[y(16) = final value of the throat erosion rate of the ablative layer thickness]*

$$a_{kk} = 0.1$$

$$ua_{kk} = 1 + a_{kk}$$

$$z_{ug} = 2 * \pi * 0.7 / \sin(15) * (\rho_{al} * s_{cc} + \rho_{abl} * s_{abl}) * (s_{abl} / 2 * ua_{kk}^2 * (R_{ex} - R_t) + ua_{kk} * (1 - a_{kk} * s_{abl} / R_t) * (R_{ex}^2 - R_t^2)/2 + a_{kk} / R_t * (s_{abl} * a_{kk} / (2 * R_t) - 1) * (R_{ex}^3 - R_t^3)/3) + \pi * (\rho_{al} * s_{cc} + \rho_{abl} * s_{abl}) * (R_{cc} + R_t + s_{abl}) * (R_{cc} - R_t)/\sin(45)$$ *[□ug = aluminium nozzle with ablative layer (diverging and converging)]*

$$z_{ug} = z_{ug} * 1.2$$

$$L_{ug} = (R_{cc} - R_t)/\sin(45) + (R_{ex} - R_t)/\sin(15) * 0.7$$

$$L_{tot} = L_{cc} + L_{ug}$$

$$L_{tot}1 = L_{tank} + L_{se} + L_{ug}$$

$s_{case} = 0.03$

$z_{case} = 100 + 225 * L_{tot} / 2.2$

$z_{case} = 450$ *[aluminium case mass calculated in two ways: constant or proportional to L_{tot}]*

$payload = y(7) * m_{conv} - z_{cc} - z_{tank} - z_{ug} - z_{case} - z_{gas} - z_{F\_res} - z_{se} - z_{O\_res}$

[$m_{conv} = m_{in}$]

Chapter 3

Code analysis and optimization

In this chapter the work done will be described, in particular all the steps necessary to achieve the optimization of the parameters and the results obtained from every simulation.

3.1 – Nominal case input values

The first step of the work, after the preliminary part (described in **Chapter 2**), is to run the *Fortran* code using the nominal input values, chosen in order to start the analysis and the subsequent optimization with a reference result.

These nominal input parameters (contained in the *input.txt* file) are chosen by *Avio* engineers and they are the reference point from which to start the study of the project.

pt_i	eps	amo1	MR_i	thrust_i	J = (At/Ap)i
[bar]				[kN]	
50	70	0.52	5.8	50	0.125

Table 6: nominal input parameters

The first trial version of the code called *o42_old.exe* was used to try the *Fortran* program and to obtain the first results given by the output window and the output files. Below the significant results are represented.

payload	Tgtf	Ltot	Gox		MR		thrust		pt		pc		time			
[kg]	[°K]	[m]	[kg/(m^2*s)]				[kN]		[bar]		[bar]		[s]			
End of last BD			min	max	min	max	min	max	min	max	min	max	start	end 1st BD	motor off	last BD
166.40	275.90	3.20	51.70	232.10	5.80	6.64	50.00	62.40	42.40	50.00	21.40	35.00	0.00	120.40	2874.80	2876.30

Table 7: simulation results for nominal case

The decision to impose *thrust_i* = 50 kN makes the sizing of the upper-stage different from the reference *Vega* one, in fact the payload is lower and all the rocket (including precedent stages) changes its specifications. All the masses involved are therefore lower, changing the target of this new *Vega* mission.

3.2 – Parametric study

The first step of the work starts with a parametric study. In fact it is necessary to try higher and lower values of every input parameter starting from the nominal value. This type of analysis is conducted two times with two different versions of the code.

In this case the code completes only one iteration for every launch and it doesn't optimize input values. It is possible imposing $r_{min} = 0$ at the launch of the code, so it does not correct the values and it stops at the first iteration directly giving the output values.

3.2.1 – Old version of the code

The first version of the code useful for the parametric study is *o42_old.exe*. The method provides the realization of a summary table where each of the six parameters is increased and decreased from the nominal value in order to observe the variation of the final results. In particular the most important output value is the payload, that must be as high as possible. Looking at the variation of the results it's possible to know how a single parameter influences the simulation.

Parametric study for z_case = 450 kg					OLD VERSION OF THE CODE			
pt_i	eps	amo1	MR_i	thrust_i	J = (At/Ap)i	payload	Tgtf	Ltot
[bar]				[kN]		[kg]	[°K]	[m]
Nominal values are yellow						End of last BD		
50	70	0.52	5.8	50	0.125	166.40	275.90	3.20
40	70	0.52	5.8	50	0.125	179.60	277.30	3.39
60	70	0.52	5.8	50	0.125	145.40	274.50	3.08
50	60	0.52	5.8	50	0.125	161.80	275.25	3.13
50	80	0.52	5.8	50	0.125	170.55	276.40	3.27
50	70	0.5	5.8	50	0.125	167.70	269.20	3.20
50	70	0.54	5.8	50	0.125	165.10	282.50	3.20
50	70	0.52	5.6	50	0.125	165.90	276.80	3.24
50	70	0.52	6	50	0.125	166.50	275.00	3.16
50	70	0.52	5.8	45	0.125	159.50	275.30	3.09
50	70	0.52	5.8	55	0.125	171.20	276.40	3.30
50	70	0.52	5.8	50	0.1	162.80	275.90	3.21
50	70	0.52	5.8	50	0.15	168.70	275.90	3.19

Table 8: parametric study o42_old.exe

In the table above the three main outputs are collected: the payload, the final temperature of the helium gas in the oxidizer tank (*Tgtf*) and the total length of the upper-stage (*Ltot*). *Ltot* is calculated by the sum only of nozzle and combustion chamber length, this because the stage is assembled putting the 4 oxidizer tanks and the 2 helium tanks sideways around (the diameter of the stage is in fact fixed at 1.9 m). Moreover the mass of the case (*z_case*), the external structure that protects the stage, is constant and fixed at 450 kg in this version of the code.

The table below represents the continuation of the upper table with the rest of the results of the study. In particular the period of time called "motor off" represents the coast arc phase.

Gox		MR		thrust		pt		pc		time			
[kg/(m^2*s)]				[kN]		[bar]		[bar]		[s]			
min	max	min	max	min	max	min	max	min	max	start	end 1st BD	motor off	last BD
51.70	232.10	5.80	6.64	50.00	62.40	42.40	50.00	21.40	35.00	0.00	120.40	2874.80	2876.30
43.10	165.80	5.80	6.30	50.00	57.55	34.40	40.00	16.80	25.00	0.00	127.65	2879.50	2881.10
60.00	298.40	5.80	6.94	50.00	67.20	50.30	60.00	25.50	45.00	0.00	113.60	2869.70	2871.10
51.70	232.10	5.80	6.63	50.00	62.20	42.20	50.00	21.40	35.00	0.00	120.20	2873.00	2874.40
51.80	232.10	5.80	6.64	50.00	62.50	42.65	50.00	21.50	35.00	0.00	120.50	2876.40	2877.80
49.60	232.10	5.80	6.62	50.00	62.10	40.00	50.00	20.60	35.00	0.00	120.90	2870.70	2872.20
53.90	232.10	5.80	6.65	50.00	62.60	45.00	50.00	22.20	35.00	0.00	120.00	2879.00	2880.40
51.90	230.70	5.60	6.40	50.00	62.50	42.80	50.00	21.60	35.00	0.00	120.30	2867.30	2868.80
51.60	233.50	6.00	6.87	50.00	62.30	42.10	50.00	21.30	35.00	0.00	120.40	2881.20	2882.70
46.60	232.10	5.80	6.70	45.00	57.10	42.20	50.00	20.30	35.00	0.00	131.90	2885.00	2886.60
56.70	232.10	5.80	6.57	55.00	67.55	42.60	50.00	22.40	35.00	0.00	110.80	2866.30	2867.60
49.40	185.65	5.80	6.64	50.00	62.30	42.45	50.00	21.40	35.00	0.00	120.50	2874.80	2876.30
53.50	278.50	5.80	6.64	50.00	62.40	42.40	50.00	21.50	35.00	0.00	120.30	2874.90	2876.30
Values calculated at the end of first BD													

Table 9: results of parametric study o42_old.exe

3.2.2 – New version of the code

After the first study, the code was modified (*o42_1.exe*) in order to have more precision during the release into the 500 km orbit. In fact it was necessary to cut thrust during the second blowdown ignition, realized by increasing the hydraulic resistance. Because of this modification the duration of the phases changed, in particular the coast arc phase (*motor off*) that became longer, and the payload decreased a bit. The table represents the changed output values for the new code version, to be compared to the old one, using nominal inputs.

Study for z_case = 450 kg					NEW VERSION OF THE CODE					
pt_i	eps	amo1	MR_i	thrust_i	J = (At/Ap)i		payload	time			
[bar]				[kN]			[kg]	[s]			
50	70	0.52	5.8	50	0.125		162.28	0.00	120.39	2935.79	2940.55
								start	end 1st BD	motor off	last BD

Table 10: new code version o42_1.exe, nominal case

The next need is to estimate a realistic value for the case mass (*z_case*), in order to have a more precise simulation, also gaining payload. In fact normally the case is not a constant structure (with a fixed mass as in the previous situation), but its geometry depends on the total length of the rocket upper-stage. *Avio* engineers proposed a way to evaluate the case mass, that is the best way to have a significant increase of the payload, but keeping at the same time a realistic estimation of the mass budget:

$$m_{case} = z_{case} = 100 + 225 * \frac{L_{tot}}{2.2}$$

The new code with this modification is called *o42_2.1.exe* and it's the final version of the code, used for the second parametric study. In the tables below the same work previously done is repeated with the new code.

Parametric study for z_case = 100 + 225*Ltot/2.2						NEW VERSION OF THE CODE		
pt_i	eps	amo1	MR_i	thrust_i	J = (At/Ap)i	payload	Tgtf	Ltot
[bar]				[kN]		[kg]	[°K]	[m]
Nominal values are yellow						End of last BD		
50	70	0.52	5.8	50	0.125	184.75	276.00	3.20
40	70	0.52	5.8	50	0.125	178.10	277.40	3.39
60	70	0.52	5.8	50	0.125	176.55	274.60	3.08
50	60	0.52	5.8	50	0.125	187.85	275.35	3.13
50	80	0.52	5.8	50	0.125	181.63	276.52	3.27
50	70	0.5	5.8	50	0.125	185.78	269.33	3.20
50	70	0.54	5.8	50	0.125	183.61	282.59	3.20
50	70	0.52	5.6	50	0.125	179.46	276.93	3.25
50	70	0.52	6	50	0.125	189.23	275.09	3.16
50	70	0.52	5.8	45	0.125	188.80	275.38	3.10
50	70	0.52	5.8	55	0.125	178.95	276.50	3.31
50	70	0.52	5.8	50	0.1	180.14	276.00	3.21
50	70	0.52	5.8	50	0.15	187.69	275.98	3.20

Table 11: new code with z_case(Ltot) o42_2.1.exe, parametric study

Gox		MR		thrust		pt		pc		time				z_case
[kg/(m^2*s)]				[kN]		[bar]		[bar]		[s]				[kg]
min	max	min	max	min	max	min	max	min	max	start	end 1st BD	motor off	last BD	
51.76	232.07	5.80	6.64	50.00	62.38	42.44	50.00	21.44	35.00	0.00	120.40	2935.80	2940.60	427.58
43.10	165.76	5.80	6.32	50.00	57.55	34.40	40.00	16.83	25.00	0.00	127.65	2952.35	2957.65	446.70
60.05	298.37	5.80	6.94	50.00	67.22	50.30	60.00	25.50	45.00	0.00	113.62	2919.29	2923.64	415.31
51.72	232.07	5.80	6.63	50.00	62.23	42.20	50.00	21.40	35.00	0.00	120.22	2935.30	2940.05	419.86
51.79	232.07	5.80	6.64	50.00	62.50	42.65	50.00	21.47	35.00	0.00	120.53	2936.19	2940.97	434.74
49.57	232.07	5.80	6.62	50.00	62.13	39.95	50.00	20.63	35.00	0.00	120.91	2938.17	2943.10	427.58
53.93	232.07	5.80	6.65	50.00	62.62	45.00	50.00	22.24	35.00	0.00	120.04	2933.36	2937.97	427.50
51.90	230.68	5.60	6.41	50.00	62.46	42.81	50.00	21.56	35.00	0.00	120.32	2943.98	2948.76	431.90
51.63	233.46	6.00	6.87	50.00	62.30	42.10	50.00	21.32	35.00	0.00	120.43	2927.94	2932.68	423.47
46.62	232.07	5.80	6.71	45.00	57.10	42.21	50.00	20.30	35.00	0.00	131.87	2939.15	2944.44	416.55
56.71	232.07	5.80	6.57	55.00	67.55	42.64	50.00	22.42	35.00	0.00	110.83	2934.27	2938.60	438.08
49.38	185.65	5.80	6.64	50.00	62.33	42.45	50.00	21.42	35.00	0.00	120.47	2935.94	2940.71	428.52
53.50	278.48	5.80	6.64	50.00	62.44	42.44	50.00	21.46	35.00	0.00	120.29	2935.60	2940.35	426.87
Values calculated at the end of first BD														

Table 12: o42_2.1.exe, parametric study results

It's possible to notice a significant increase of the payload, while *Ltot* is the same of the previous case. However its value is a bit high but this problem will be solved with the optimization, in fact the code will tend to decrease the total length (*Ltot*) in order to decrease the case mass (*z_case*), gaining many kilograms for the payload.

3.3 – Optimization work

Starting from the code previously used for the parametric study, now it's necessary to optimize some selected input values so that the results should be the best possible. The code can do this automatically if it receives in input r_{min} > 0 at the launch. In this case every iteration of the code corrects the parameters chosen to maximize the payload. If the value of r_{min} is very low (between 0.01 and 0.1) the code will need more iterations to arrive at convergence but it will reach the best result without errors.

This process of optimization is not fast, but it needs some steps to be concluded. In fact it is necessary to begin with only 2 input values to be optimized, then move on to 3 inputs and in the end 4. The final input files generated from the optimization with 2 parameters will be used to start the 3 inputs optimization and so on. This method is useful to minimize errors and to converge faster, in fact the choice of correct inputs is fundamental to avoid that the code gets stuck or conducts to incorrect results. A work like this is possible with a modification of the main *Fortran* code (*oN2.for* where N is the number of optimized inputs), where the parameters to be optimized are introduced like in the image below, while the other are commented.

```
PAR(1)='RM iniziale'
YPMIN(1)=1.D0
YPMAX(1)=3.d0
YP(1)=RMI
PAR(2)='epsilon'
YPMIN(2)=10.D0
YPMAX(2)=20.d0
YP(2)=eps
PAR(3)='At/Ap iniziale'
YPMIN(3)=0.1d0
YPMAX(3)=0.3d0
YP(3)=atapi
PAR(4)='pti'
YPMIN(4)=3.d0
YPMAX(4)=6.d0
YP(4)=pti/1.d6
```

Figure 14: portion of script oN2.for, parameters optimization

At this point it's possible to compile the code generating the executable (*oN2.exe*). The results obtained from the optimization are shown below. Only two input parameters are fixed at the nominal value, because they give the

best payload (in the tables are reported also other values of *thrust_i* only to demonstrate this):

- *thrust_i* = 50 kN; this value is imposed to resize the new *Vega* rocket with a smaller payload.
- *amo1* = 0.52 can't be an optimization variable because it may lead to very small values of regression rate at the end of motor operation.

Optimization work: o22.exe							z_case = 100 + 225*Ltot/2.2		
pt_i	eps	amo1	MR_i	thrust_i	J = (At/Ap)i		payload	Tgtf	Ltot
[bar]				[kN]			[kg]	[°K]	[m]
Parameters optimized after iterations are blue							End of last BD		
50	39.7	0.52	7.78	50	0.125		213.52	265.87	2.65
50	34.4	0.52	8.02	60	0.125		212.18		2.71
50	48.9	0.52	7.49	40	0.125		207.96		2.60

Gox		MR		thrust		pt		pc		time				z_case
[kg/(m^2*s)]				[kN]		[bar]		[bar]		[s]				[kg]
min	max	min	max	min	max	min	max	min	max	start	end 1st BD	motor off	last BD	
50.80	245.29	7.78	8.86	50.00	61.25	38.63	50.00	20.35	35.00	0.00	119.69	2872.21	2876.76	370.88

Table 13: o22.exe

o22.exe optimizes only 2 parameters:

- $\varepsilon_i = \frac{A_{ex}}{A_{t_i}}$
- MR_i = initial mixture ratio

Optimization work: o32.exe							z_case = 100 + 225*Ltot/2.2		
pt_i	eps	amo1	MR_i	thrust_i	J = (At/Ap)i		payload	Tgtf	Ltot
[bar]				[kN]			[kg]	[°K]	[m]
Parameters optimized after iterations are blue							End of last BD		
50	39.80	0.52	7.76	50	0.333		223.10	265.79	2.63
50	34.96	0.52	7.94	60	0.360		224.45	265.52	2.69
50	50.39	0.52	7.45	40	0.301		215.06		2.59

Gox		MR		thrust		pt		pc		time				z_case
[kg/(m^2*s)]				[kN]		[bar]		[bar]		[s]				[kg]
min	max	min	max	min	max	min	max	min	max	start	end 1st BD	motor off	last BD	
58.61	652.90	7.76	8.90	50.00	62.10	38.60	50.00	20.63	35.00	0.00	118.29	2869.84	2874.31	368.65
72.37	709.72	7.94	8.94	60.00	72.39	38.50	50.00	22.25	35.00	0.00	100.55	2852.81	2856.50	375.44

Table 14: o32.exe

Introducing the third parameter J_i in the *o32.exe* the payload increases.

The next step is necessary to optimize p_{ti} maintaining constant MR_i and J_i at the best values found. This intermediate step (*o22bis.exe*) is useful because the next optimization with four parameters needs coherent inputs to start from, avoiding errors (in fact both epsilon and tank pressure decrease a lot while the payload increases).

Optimization work: o22bis.exe						z_case = 100 + 225*Ltot/2.2		
pt_i	eps	amo1	MR_i	thrust_i	J = (At/Ap)i	payload	Tgtf	Ltot
[bar]				[kN]		[kg]	[°K]	[m]
Parameters optimized after iterations are blue						End of last BD		
32.35	21.04	0.52	7.76	50	0.333	243.03	265.41	2.62
33.71	20.36	0.52	7.94	60	0.360	241.69		2.70
30.85	21.91	0.52	7.45	40	0.301	236.72		2.55

Gox		MR		thrust		pt		pc		time				z_case
[kg/(m^2*s)]				[kN]		[bar]		[bar]		[s]				[kg]
min	max	min	max	min	max	min	max	min	max	start	end 1st BD	motor off	last BD	
44.56	323.58	7.51	8.15	46.23	53.75	24.88	32.35	12.08	17.35	0.00	129.75	2903.75	2909.18	367.86

Table 15: o22bis.exe

Optimization work: o42.exe						z_case = 100 + 225*Ltot/2.2		
pt_i	eps	amo1	MR_i	thrust_i	J = (At/Ap)i	payload	Tgtf	Ltot
[bar]				[kN]		[kg]	[°K]	[m]
Parameters optimized after iterations are blue						End of last BD		
30.67	18.98	0.52	8.11	50	0.569	247.80	263.82	2.56

Gox		MR		thrust		pt		pc		time				z_case
[kg/(m^2*s)]				[kN]		[bar]		[bar]		[s]				[kg]
min	max	min	max	min	max	min	max	min	max	start	end 1st BD	motor off	last BD	
47.20	504.24	7.81	8.52	45.92	53.86	23.24	30.67	11.21	15.70	0.00	128.65	2896.19	2901.49	361.53

Table 16: o42.exe

The 4 parameters optimization with the code *o42.exe* gives the best results but the value $J_i = 0.569$ is too high. In fact this may cause a too high value of Mach number in the port area, causing large pressure losses and nonuniform grain regression. So the decision is to fix the value of $J_i = 0.4$ (Mach ~ 0.3 at the grain exit) and conclude the optimization study with 3 parameters (p_{ti}, ε and MR_i). Final results are reported below.

Optimization work: o32new.exe							z_case = 100 + 225*Ltot/2.2		
pt_i	eps	amo1	MR_i	thrust_i	J = (At/Ap)i		payload	Tgtf	Ltot
[bar]				[kN]			[kg]	[°K]	[m]
Parameters optimized after iterations are blue							End of last BD		
31.61	20.23	0.52	8.22	50	0.400		245.57	263.83	2.56
33.10	19.76	0.52	8.35	60	0.400		243.51		2.64

Gox		MR		thrust		pt		pc		time				z_case
[kg/(m^2*s)]				[kN]		[bar]		[bar]		[s]				[kg]
min	max	min	max	min	max	min	max	min	max	start	end 1st BD	motor off	last BD	
42.27	376.52	7.89	8.61	45.72	53.60	23.95	31.61	11.61	16.61	0.00	129.59	2894.75	2900.08	361.98

Table 17: o32new.exe final results

The optimization procedure can be considered concluded and the final results can be analysed in the next section.

3.4 – Results

Tables and charts below represent the significant values of the hybrid rocket motor of the upper-stage. All this is obtained from the code output files, handled by a *MATLAB* code which collects all the results and plots the charts. This *MATLAB* code is attached in the section **Appendix A**.

MASS BUDGET [kg]	payload	245.57
	propellant (mp)	2420.00
	residual fuel	27.36
	residual ox	151.24
	mp/(mp+ms)	0.853
	gas He	8.27
	ox tank	56.50
	gas tank	28.01
	nozzle	95.34
	cc	49.09
	case	362.00
	structure (ms)	415.81
	final mass	1023.38

Table 18: mass budget

$$m_s = m_{O_{res}} + m_{F_{res}} + m_{He} + m_t + m_{gt} + m_n + m_{cc}$$

$$m_{fin} = m_{payload} + m_s + m_{case}$$

PERFORMANCE VALUES	Dt iniz [mm]	145.97
	Dt fin [mm]	168.76
	D_ex [mm]	656.51
	eps fin	15.13
	eps iniz	20.23
	MR avg	8.33
	t (1st burn) [s]	129.59
	prop. flow avg [kg/s]	18.46
	thrust avg [kN]	51.57
	I_sp avg [s]	285.02
	web [m]	0.207
	L/d	1.35

Table 19: performance values

Below are reported the charts with the trend of the main parameters. The time matches the first burn until the end of the first blowdown. It's easy to see the point where the p_t=cost phase ends and the blowdown starts (rapid decrease).

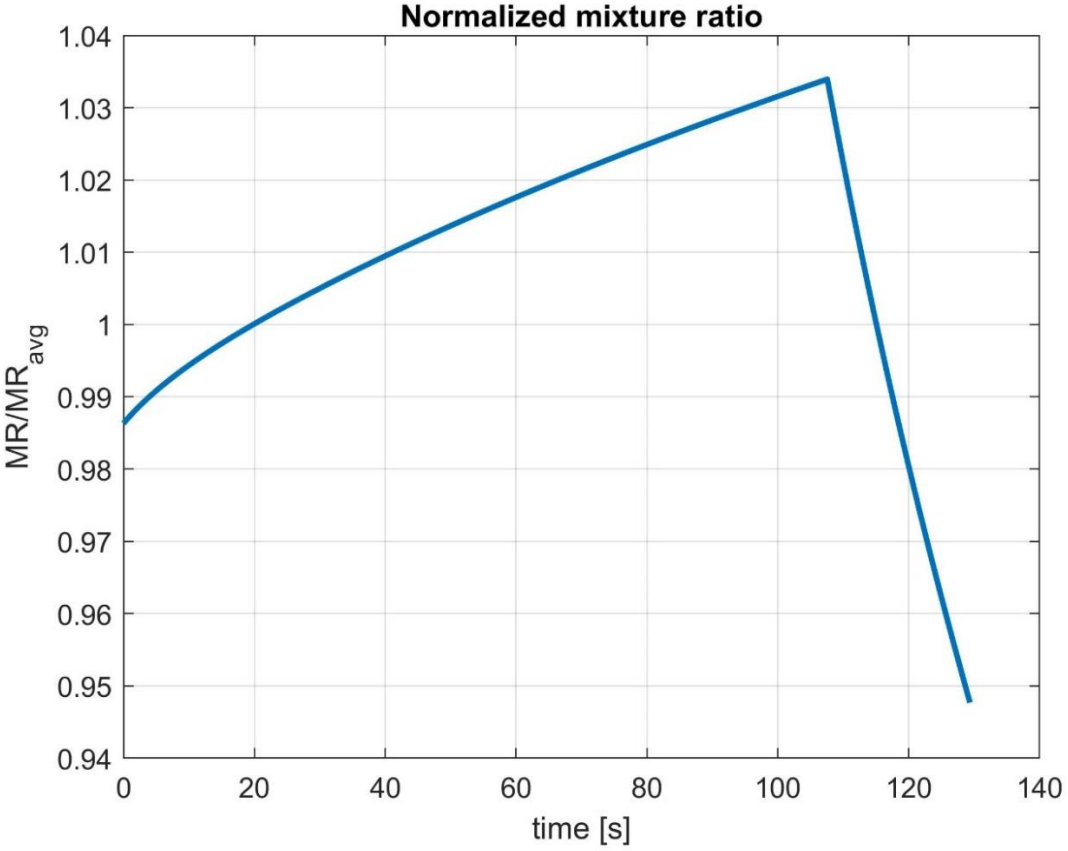
Normalized mixture ratio
MR/MR_avg
1.04
1.03
1.02
1.01
1
0.99
0.98
0.97
0.96
0.95
0.94
0
20
40
60
80
100
120
140
time [s]

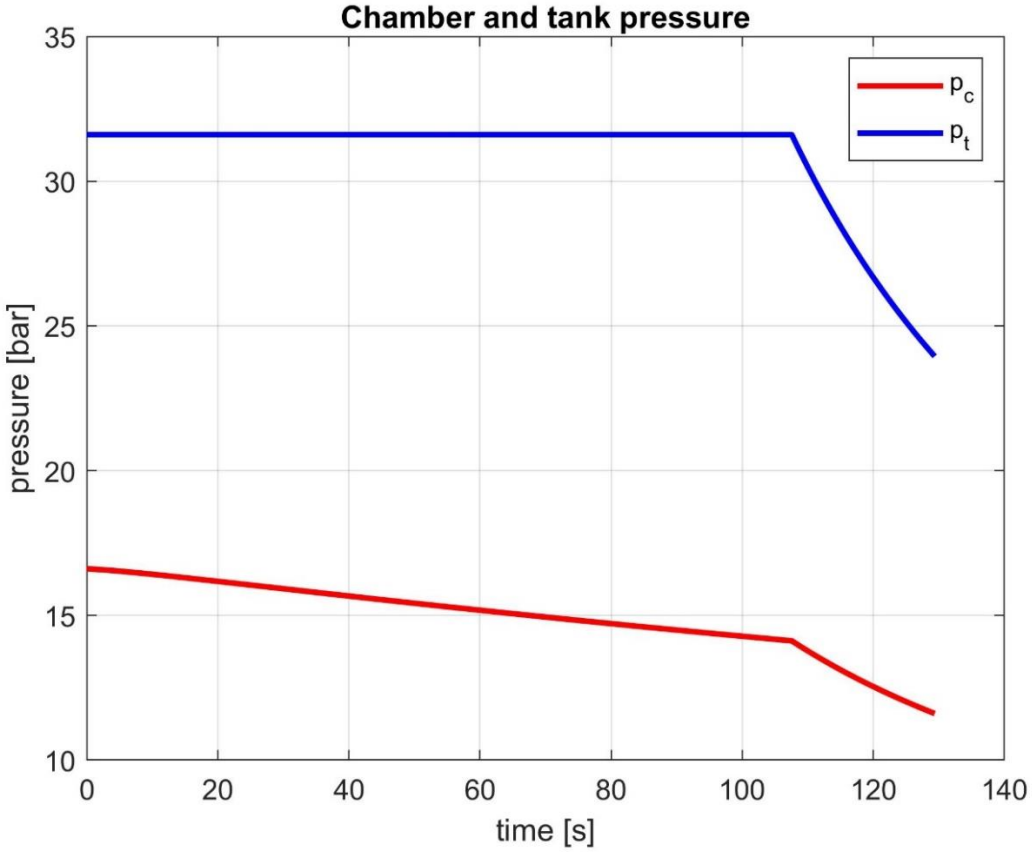
Chamber and tank pressure
pressure [bar]
35
30
25
20
15
10
p_c
p_t
0
20
40
60
80
100
120
140
time [s]

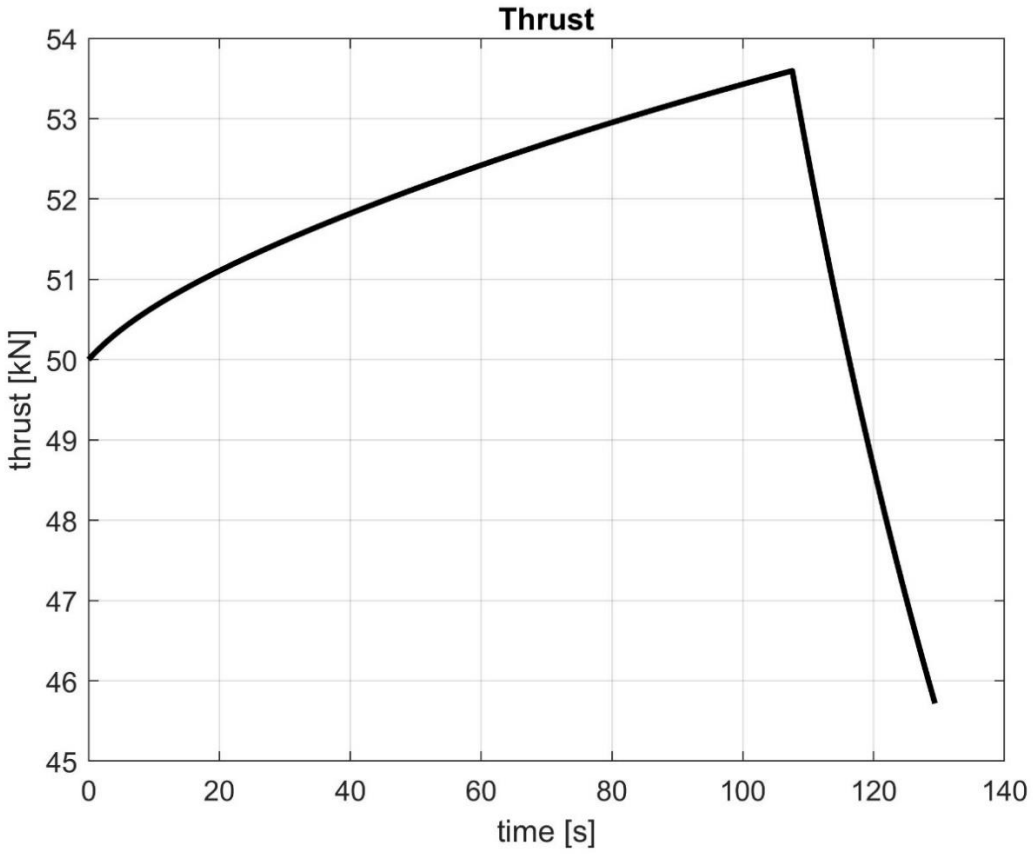
Thrust
thrust [kN]
time [s]
54
53
52
51
50
49
48
47
46
45
0
20
40
60
80
100
120
140

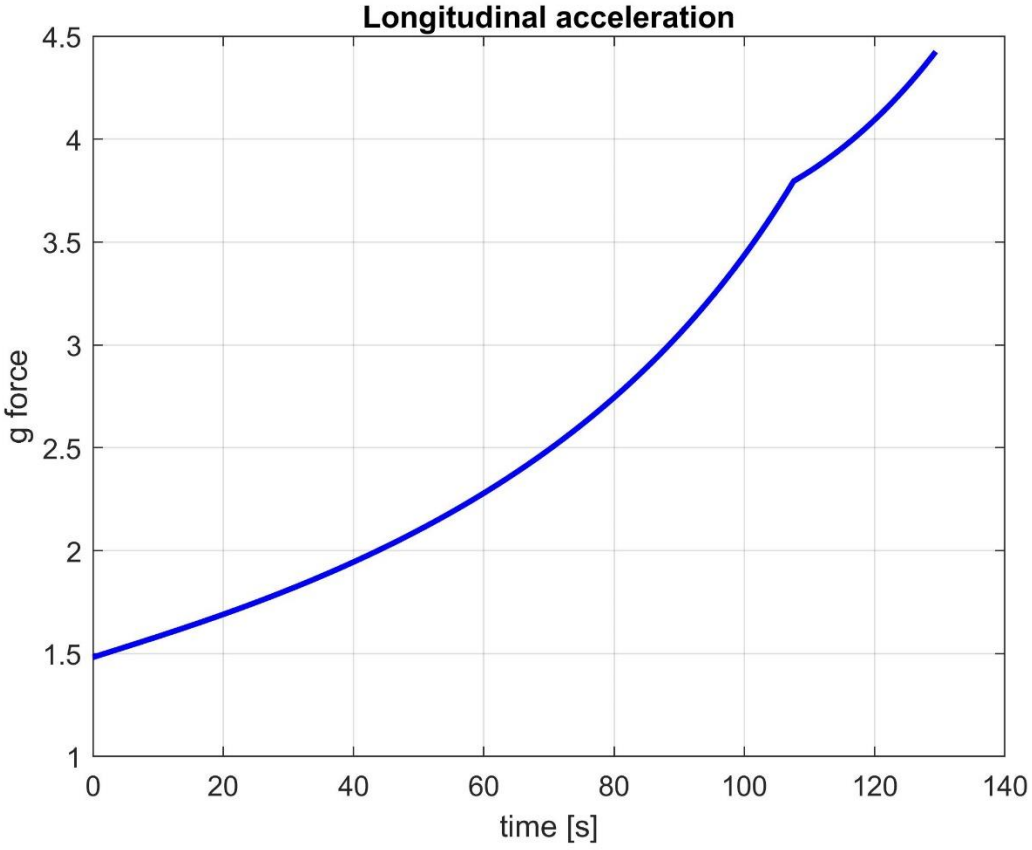
Longitudinal acceleration
g force
time [s]
4.5
4
3.5
3
2.5
2
1.5
1
0
20
40
60
80
100
120
140

The “Longitudinal acceleration” chart demonstrates the respect of the constraint not to exceed 5.5 g (the limit of *Vega* launcher [2]).

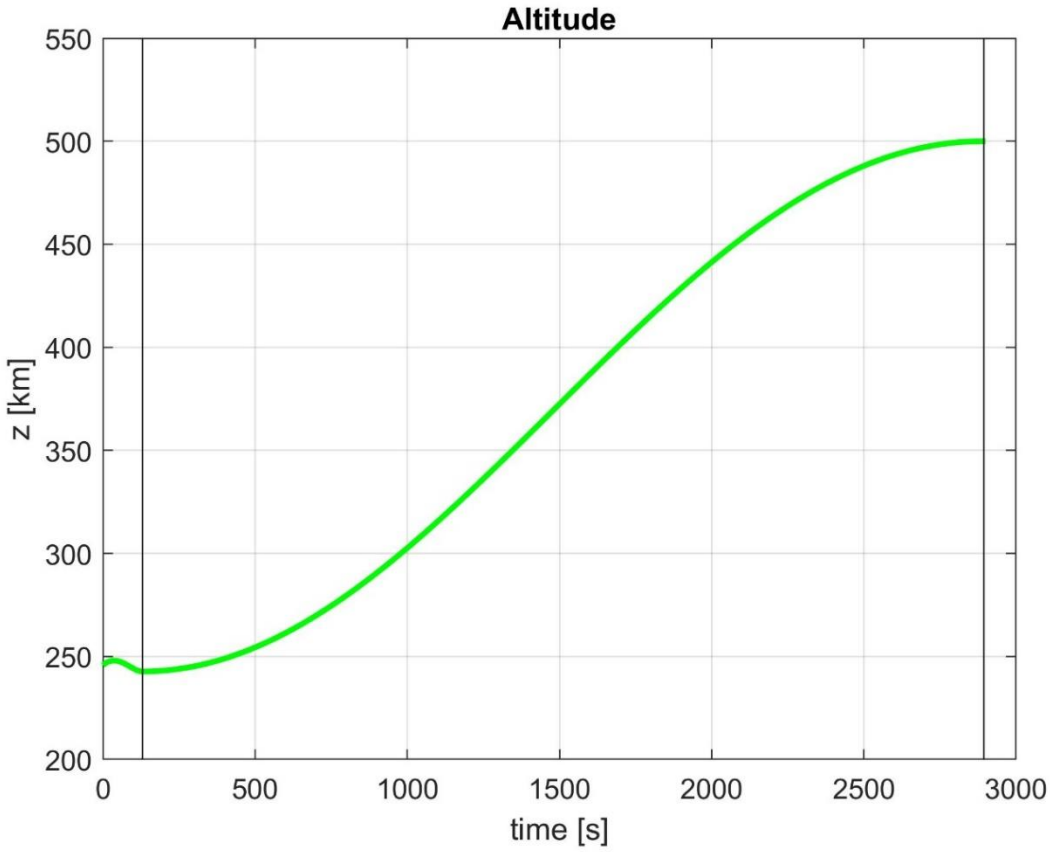

In the altitude chart the time contained between the two black vertical lines represents the coast arc phase, when the motor is turned off. The last blowdown (with a small duration) is not clearly visible.

Conclusions

The choice to implement a hybrid rocket motor on an upper-stage for small launchers present an appealing application. The realization of this particular solution is analysed through a coupled optimization of motor design (direct procedure) and trajectory (indirect) in order to maximize the payload inserted into the final orbit. This is a fundamental step to create a next equal comparison with the corresponding upper-stages realized with solid/liquid solutions.

The typical disadvantages of HRMs, like low regression rate and mixture ratio shifting, can be limited with a complete analysis and optimization of the whole motor burning during every single phase and the choice of a suitable propellant combination like H_2O_2/wax. In fact a solid hydrocarbon type fuel (wax/paraffin) allows the adoption of a single-port grain, avoiding issues related to multiport grains, due to its high regression rate. Also the choice of H_2O_2 as liquid oxidizer can give advantages like high density, easy storability and non-cryogenic necessity (as LOX), although losing a bit of performance.

The main necessity of a HRM to be competitive is the maintenance of the overall system simplicity with respect to LREs. In particular the feed system, which has only the oxidizer line, is implemented with partially regulated tank pressure (instead of turbopumps), allowing to obtain an optimal performance and saving weight. Also the absence of throttle regulation is strategic because it guarantees simplicity and lightness, but however permitting the possibility of shut-off and reignition (impossible with SRMs).

With respect to the original *Vega* mission (payload 1500 kg, altitude 700 km) this simulation has a lower upper-stage initial thrust value imposed to 50 kN, so the final optimal payload mass is evaluated to be 245.57 kg, obviously much smaller. As the new mission is different, both for components' masses decrease and substitution of two stages (solid and liquid) with only one hybrid, it's difficult to make a direct comparison with *Vega*. This type of confrontation is studied in reference paper [3], that implement exactly the original Vega mission with a HRM upper-stage.

The main conclusion of the thesis work is that the realization of a small launcher with a hybrid upper-stage is a valid solution simple and cheap, which can be optimized for the application on future launchers.

Appendix A

The *MATLAB* code useful for the handling of final results is reported below.

```
fid4 = fopen('output4.txt','r');
fid7 = fopen('output7.txt','r');
fid6 = fopen('output6.txt','r');
fid8 = fopen('output8.txt','r');

A = fscanf(fid4,'%f',[3,inf]);
B = fscanf(fid7,'%f',[4,inf]);
C = fscanf(fid6,'%f',[4,inf]);
D = fscanf(fid8,'%f',[4,inf]);

t = A(1,:);     %time array
RM = A(2,:);    %mixture ratio array
S = A(3,:);     %thrust array
RMmax = max(RM);
RMmin = min(RM);
Smax = max(S)*10;
Smin = min(S)*10;

Gox = B(3,:);
Gox_max = max(Gox);
Gox_min = min(Gox);

pt = C(2,:);
pc = C(3,:);
pt_max = max(pt);
pt_min = min(pt);
pc_max = max(pc);
pc_min = min(pc);
```

```

res = [Gox_min Gox_max RMmin RMmax Smin Smax pt_min pt_max pc_min pc_max]
%all the results of tables in order

a=0;
for i = 1:length(t)-1
    spinta(i) = (S(i)+S(i+1))/2;  %average thrust in a single time interval
    tempo(i) = t(i+1)-t(i);
    a= a + spinta(i)*tempo(i);
end
S_avg = a/129.59        %average thrust

figure
plot(t,RM./8.33,'linewidth',2)
xlabel('time [s]')
ylabel('MR/MR_a_v_g')
title('Normalized mixture ratio')
grid on
print('MR.jpg','-djpeg','-r400')

figure
plot(C(1,:),pc,'r','linewidth',2)
hold on
plot(C(1,:),pt,'b','linewidth',2)
xlabel('time [s]')
ylabel('pressure [bar]')
title('Chamber and tank pressure')
legend('p_c','p_t')
```

```
grid on
print('pressure.jpg','-djpeg','-r400')

figure
plot(t,S*10,'k','linewidth',2)
xlabel('time [s]')
ylabel('thrust [kN]')
title('Thrust')
grid on
print('spinta.jpg','-djpeg','-r400')

figure
plot(D(1,:),D(2,:),'g','linewidth',2)
hold on
plot([129.59 129.59],[200 550],'k')
plot([2894.75 2894.75],[200 550],'k')
xlabel('time [s]')
ylabel('z [km]')
title('Altitude')
grid on
print('quota.jpg','-djpeg','-r400')

m_fuel = B(2,:)./RM;          %fuel mass flow array
portata = B(2,:)+m_fuel;      %propellant mass flow array
```

```
a = 3443.37;                  %total initial rocket mass
massa_tot(1) = a;
for i = 1:length(RM)-1
    port_med(i) = (portata(i)+portata(i+1))/2;
    tempo(i) = t(i+1)-t(i);
    a = a - port_med(i)*tempo(i);   %rocket mass progressive decreasing during operation
    massa_tot(i+1) = a;
end

T_M = S*10000./massa_tot/9.8;       %longitudinal acceleration (g) on the rocket

figure
plot(t,T_M,'b','linewidth',2)
xlabel('time [s]')
ylabel('g force')
title('Longitudinal acceleration')
grid on
print('g force.jpg','-djpeg','-r400')

fclose(fid4);
fclose(fid7);
fclose(fid6);
```

Bibliography

[1] Paweł Surmacz, Grzegorz Rarata, “Hybrid Rocket Propulsion Development and Application”, Institute of Aviation, Al. Krakowska 110/114, 02-256 Warsaw, Poland, 2009.

[2] Isakowitz S. J., Hopkins J. A., Hopkins J. A. Jr., “International Reference Guide to Space Launch Systems”, 4th ed., AIAA, Reston, VA, 2004, pp. 517–524.

[3] Casalino L., Letizia F., Pastrone D., “Optimization of Hybrid Upper-Stage Motor with Coupled Evolutionary/Indirect Procedure”, Politecnico di Torino, 10129 Torino, Italy, *Journal of Propulsion and Power*, Vol. 30, No. 5, 2014.

[4] Humble Ronald, Gary Henry, Larson Wiley, “Space Propulsion Analysis and Design”, McGraw-Hill, 1995.

[5] Sharp Tim, “SpaceShipOne: The First Private Spacecraft”, 2019, (https://www.space.com/16769-spaceshipone-first-private-spacecraft.html).

[6] Pastrone D., Casalino L., Dispense del corso *Endoreattori*, Politecnico di Torino, 2018.

[7] Lentini D., Dispense del corso di *Endoreattori*, Università degli Studi di Roma “La sapienza”, 2001.

[8] https://www.narom.no/undervisningsressurser/sarepta/rocket-theory/rocket-engines/the-engine-types-solid-liquid-and-hybrid-and-a-fourth/

[9] https://sites.google.com/site/pennhybridrocket/how-do-hybrid-rocket-motors-work

[10] Cantwell B. J., “Aircraft and Rocket Propulsion”, 2019.

[11] https://www.avio.com/vega

[12] https://www.arianespace.com/vehicle/vega/

[13] http://www.esa.int/Enabling_Support/Space_Transportation/Launch_vehicles/Vega

[14] Tariq Malik, "Europe Launches New Vega Rocket on Maiden Voyage", Space.com, 2012.

[15] Svitak Amy, "European Vega Small-Class Launcher Targets Government Market", Aviation Week, 2014.

[16] "Expendable Launch Vehicles", spacetethers.com, 2018.

[17] Caporicci M., "The Future of European Launchers: The ESA Perspective", *European Space Agency*, 2000.

[18] "Solid propellant rocket stage", astronautix.com, *Encyclopedia Astronautic*a, 2013.